Received: 9 July 2020 | Revised: 1 December 2020 | Accepted: 5 January 2021

DOI: 10.1002/hbm.25358

RESEARCH ARTICLE

WILEY

Structural control energy of resting-state functional brain states reveals less cost-effective brain dynamics in psychosis vulnerability

Daniela Zöller[1,2,3,4] | Corrado Sandini[3] | Marie Schaer[3] | Stephan Eliez[3] | Danielle S. Bassett[5,6,7,8,9] | Dimitri Van De Ville[1,2]

[1]Medical Image Processing Laboratory, Institute of Bioengineering, École Polytechnique Fédérale de Lausanne (EPFL), Lausanne, Switzerland

[2]Department of Radiology and Medical Informatics, University of Geneva, Geneva, Switzerland

[3]Institute of Neuromodulation and Neurotechnology, University of Tübingen, Tübingen, Germany

[4]Developmental Imaging an Psychopathology Laboratory, Department of Psychiatry, University of Geneva, Geneva, Switzerland

[5]Department of Bioengineering, University of Pennsylvania, Philadelphia, Pennsylvania

[6]Department of Electrical & Systems Engineering, University of Pennsylvania, Philadelphia, Pennsylvania

[7]Department of Neurology, University of Pennsylvania, Philadelphia, Pennsylvania

[8]Department of Physics & Astronomy, University of Pennsylvania, Philadelphia, Pennsylvania

[9]Department of Psychiatry, University of Pennsylvania, Philadelphia, Pennsylvania

Correspondence
Daniela Zöller, Medical Image Processing Laboratory, Institute of Bioengineering, École Polytechnique Fédérale de Lausanne (EPFL), Lausanne, Switzerland.
Email: daniela.zoeller@uni-tuebingen.de

Funding information
Alfred P. Sloan Foundation; Army Research Laboratory, Grant/Award Number: W911NF-10-2-0022; Army Research Office, Grant/Award Numbers: Bassett-W911NF-14-1-0679, DCIST- W911NF-17-2-0181, W911NF-16-1-0474; ISI Foundation; John D. and Catherine T. MacArthur Foundation; National Center of Competence in Research (NCCR) "SYNAPSY - The Synaptic Bases of Mental Diseases", Grant/Award Numbers: 51AU40-125759, 51NF40-158776, 51NF40-185897; National Institute of Child Health and Human Development, Grant/Award Number: 1R01HD086888-01; National Institute of Mental Health, Grant/Award Numbers: 2-R01-DC-009209-11, R01-MH107235, R01-MH112847, R21-M MH-106799; National Institute of Neurological Disorders and Stroke, Grant/Award Number: R01 NS099348; National Science Foundation, Grant/Award Numbers: BCS-1430087, BCS-1441502, BCS-1631550, NSF PHY-1554488;

Abstract

How the brain's white-matter anatomy constrains brain activity is an open question that might give insights into the mechanisms that underlie mental disorders such as schizophrenia. Chromosome 22q11.2 deletion syndrome (22q11DS) is a neurodevelopmental disorder with an extremely high risk for psychosis providing a test case to study developmental aspects of schizophrenia. In this study, we used principles from network control theory to probe the implications of aberrant structural connectivity for the brain's functional dynamics in 22q11DS. We retrieved brain states from resting-state functional magnetic resonance images of 78 patients with 22q11DS and 85 healthy controls. Then, we compared them in terms of persistence control energy; that is, the control energy that would be required to persist in each of these states based on individual structural connectivity and a dynamic model. Persistence control energy was altered in a broad pattern of brain states including both energetically more demanding and less demanding brain states in 22q11DS. Further, we found a negative relationship between persistence control energy and resting-state activation time, which suggests that the brain reduces energy by spending less time in energetically demanding brain states. In patients with 22q11DS, this behavior was less pronounced, suggesting a deficiency in the ability to reduce energy through brain activation. In summary, our results provide initial insights into the functional

Paul Allen Foundation; Schweizerischer Nationalfonds zur Förderung der Wissenschaftlichen Forschung, Grant/Award Numbers: 145250, 163859, 234730_144260, 32473B_121966

implications of altered structural connectivity in 22q11DS, which might improve our understanding of the mechanisms underlying the disease.

KEYWORDS
22q11.2 deletion syndrome, brain state dynamics, diffusion MRI, network control energy, resting-state functional MRI

1 | INTRODUCTION

The brain is a complex dynamic system and brain function during rest and task can be described in terms of the dynamic activation and interaction of different *brain states*: sets of brain regions that are coherently activating and deactivating (Karahanoğlu & Van De Ville, 2017; Preti, Bolton, & Van De Ville, 2017). More specifically, healthy brain function is characterized by continuous transitions between different cognitive states (as e.g., the internally oriented default mode network (DMN), or the attention-related fronto-parietal network (FPN)), and alterations in these dynamic state transitions could inform on disrupted brain function in mental diseases (Christoff, Irving, Fox, Spreng, & Andrews-Hanna, 2016). How the brain's underlying structural backbone constrains and facilitates this dynamic behavior is an intensively studied question in the neuroscience community (Bassett & Sporns, 2017; Becker et al., 2018; Honey et al., 2009). The joint consideration of structural and functional properties is particularly promising to provide a better mechanistic explanation of the causes that underlie brain disorders such as schizophrenia (Braun et al., 2018). In recent years, approaches for the investigation of dynamic properties have proven to be particularly useful in probing brain function in health and disease (Karahanoğlu & Van De Ville, 2017; Preti et al., 2017; Van Den Heuvel & Fornito, 2014). Schizophrenia, in particular, is—as an extension of the well-accepted dysconnectivity hypothesis (Friston, Brown, Siemerkus, & Stephan, 2016)—increasingly perceived as a disorder of broad alterations in large-scale brain state dynamics (Braun et al., 2016; Du et al., 2016; Fornito, Zalesky, Pantelis, & Bullmore, 2012). As schizophrenia, and mental disorders in general, have a polygenetic basis in combination with strong social-environmental and developmental implications, they are likely also affecting a multitude of biological systems (Braun et al., 2018). Thus, a better insight on how the alterations in the brain's structure may lead to aberrant dynamic activation would improve our understanding of this disease to ultimately improve clinical management and patient outcomes (Braun et al., 2018).

Network control theory provides a framework to address this question of structure–function relationship, and to analyze how the brain's structural topology influences its dynamic function (Betzel, Gu, Medaglia, Pasqualetti, & Bassett, 2016; Gu et al., 2015; Gu et al., 2017; Karrer et al., 2020; Kim et al., 2018). While initial studies of the relationship between brain structure and function used cross-modal correlations (Honey et al., 2009), network control theory approaches aim to mechanistically describe how brain structure affects its function (Bassett & Sporns, 2017; Braun et al., 2018). In network control theory approaches, the brain is modeled as a graph defined by its structural connectivity, where nodes correspond to brain regions, and edges indicate structural connectivity strength between brain regions. The state of this system is defined by the neurophysiological activation of each brain region, and a (usually linear) dynamic model describing the dynamic transition between these functional brain states over time. Under the assumption that the brain's state is controlled through an internal or external control input signal, it is then possible to quantify how the underlying structural architecture facilitates or constrains the system's dynamic behavior. In other words, the measured brain state at one moment (in terms of hemodynamic activation) is modeled as the propagated activation during an earlier brain state and an added control input at the control regions. This assumption is the basis for many models of information propagation in the brain (Srivastava et al., 2020) and the validity of this view is supported by empirical evidence showing that regional fMRI activation levels during task can accurately be predicted by flow of activity between brain regions (Cole, Ito, Bassett, & Schultz, 2016). Through this framework, network control theory can be used to investigate how much energy the brain would require (i.e., how high the control input would be) to steer itself into different cognitive states (through internal control inputs; Betzel et al., 2016; Gu et al., 2015), or to identify the most promising targets for neurostimulation to control the brain's state (through external control inputs; Khambhati et al., 2019; Muldoon et al., 2016).

Of note, the network control theory allows to examine the control energy that is required for specific trajectories between a precisely defined initial state and a precisely defined target state. A simple intuitive example of such a state transition is the transition from activation of the DMN to activation of the FPN (Betzel et al., 2016; Gu et al., 2017; Kim et al., 2018). The initial and target states can either be defined by an atlas (Cui et al., 2020; Gu et al., 2017), or by data-driven brain states retrieved from functional magnetic resonance imaging (fMRI) (Braun et al., 2019; Cornblath et al., 2020). By defining identical initial state and target state, one can obtain the control energy that would be required to *persist* in any particular brain state (Cornblath et al., 2020). Despite it's simplifying assumptions, the network control theory framework has the advantage that it allows to go beyond a purely correlative description of structure–function relationships and integrate functional and structural properties in a common model, without the use of more complex and computationally demanding generative models as for example (Deco et al., 2018; Ghosh, Rho, McIntosh, Kötter, & Jirsa, 2008;

Kringelbach et al., 2020). A validation of the model was provided in a recent study that compared network control energy to brain state transition probabilities during rest and during an *n*-back working memory task (Cornblath et al., 2020). The authors of the study found a negative relationship between control energy and transition probability during rest, which supports that the linear diffusion of brain activity on the brain's structural white matter connections indeed constrains brain state transitions at rest (Cornblath et al., 2020). Of note, while brain activity can also lead to a change in structure; for example, through neural plasticity, in the network control theory framework used in this way, the network structure is fixed in order to investigate the cost of dynamic changes in activation that happen on top of this network (Bassett & Sporns, 2017; Bassett, Zurn, & Gold, 2018).

Studies in healthy and clinical populations have demonstrated that network controllability measures can provide characteristic profiles for different cognitive brain systems (Gu et al., 2015), change with development (Cui et al., 2020; Tang et al., 2017), are a reliable and heritable property of the structural connectome (Lee, Rodrigue, Glahn, Bassett, & Frangou, 2020), and track individual profiles in cognitive functions (Lee et al., 2020), executive functions (Cui et al., 2020), and impulsivity (Cornblath et al., 2018). Additionally, controllability properties relate to different neurotransmitter profiles (Shine et al., 2019) and are promising to guide target selection for neurostimulation (Khambhati et al., 2019; Muldoon et al., 2016). Persistence control energy in healthy subjects was found to be significantly lower when computed for structural brain networks than for random null models preserving topology and spatial constraints, suggesting that the brain's structural wiring promotes persistence in functional brain states at low energy cost (Cornblath et al., 2020). In patients with temporal lobe epilepsy, controllability was found to be reduced suggesting a lower range of functional dynamics (Bernhardt et al., 2019), and in patients with bipolar disorder aberrant structural connectivity in fronto-limbic subnetworks leads to altered controllability (Jeganathan et al., 2018). In patients with schizophrenia, the persistence control energy of a data-driven working memory brain state was found to be higher compared to healthy control subjects, which was interpreted as reduced stability of this brain state in patients (Braun et al., 2019). Further, this study also found evidence supporting that persistence control energy is modulated by dopamine D1 receptor expression, whereas dopamine D2 receptor expression was modulating control energy for brain state transitions.

When brain states are derived from fMRI, network control theory allows to directly compare the temporal properties of these brain states (measured during fMRI) with the persistence control energy that would be needed to engage in these same brain states based on structural connectivity (measured with diffusion weighted MRI; Cornblath et al., 2020). In this way, it is possible to investigate if the predicted effect of aberrant structural brain architecture on brain dynamics (reflected by persistence control energy) is in line with the measured temporal activation during rest. In the present study, we use this framework in order to explore whether and how such an integration of network control theory with dynamic functional brain state analysis could highlight a disruption of structure–function relationship, which in turn might contribute vulnerability to psychiatric disorders. To this aim we investigated individuals with 22q11.2 deletion syndrome (22q11DS), a neurodevelopmental disorder characterized, characterized by a heightened genetic risk for development of psychopathology (McDonald-McGinn et al., 2015). Indeed, individuals with 22q11DS, are characterized by an approximately 30% risk of developing schizophrenia (Schneider et al., 2014) along with extremely elevated rates of mood disorders, anxiety disorders and attention-deficit hyperactivity disorders (McDonald-McGinn et al., 2015). Moreover, individuals with 22q11DS are typically diagnosed at a young age and irrespective of their psychiatric phenotype, offer the unique opportunity of investigating vulnerability mechanisms that predate the onset of full-blown psychopathology (Bassett & Chow, 1999; Insel, 2010).

In 22q11DS, the white matter microstructure and connectivity has been extensively studied, mostly in terms of whole-brain or tract-based diffusivity properties (reviewed in Scariati, Padula, Schaer, & Eliez, 2016). Affected white-matter bundles mostly include long-range frontal-frontal, frontal-occipital, and fronto-parietal connections (Kikinis et al., 2016; Olszewski et al., 2017; Roalf et al., 2017; Scariati et al., 2016; Tylee et al., 2017). Only a few studies have thus far examined the characteristics of structural whole-brain networks (Kikinis et al., 2013; Ottet, Schaer, Cammoun, et al., 2013; Ottet, Schaer, Debbané, et al., 2013; Padula et al., 2017; Váša et al., 2016; Zhan et al., 2018), also mostly reporting fronto-temporal, fronto-parietal (Ottet, Schaer, Cammoun, et al., 2013; Ottet, Schaer, Debbané, et al., 2013; Zhan et al., 2018), and limbic dysconnectivity (Ottet, Schaer, Cammoun, et al., 2013; Padula et al., 2015). From a topological perspective, Ottet et al. reported longer path lengths and disconnectivity of the brain's hub regions, specifically, in the frontal lobes (Ottet, Schaer, Debbané, et al., 2013), and Váša et al. (2016) uncovered a "de-centralization" in 22q11DS with a rerouting of shortest network paths to circumvent an affected core that included frontal, parietal, and subcortical regions. FMRI studies in 22q11DS have so far mostly focused on static properties. In the only three studies who looked at dynamic features of resting-state brain function, we found global reductions in variability of blood-oxygenation level dependent (BOLD) signals (Zöller, Schaer, et al., 2017), and reduced BOLD variability in the dorsal anterior cingulate cortex (a central node of the salience network [SN]) in relationship to higher positive psychotic symptoms (Zöller, Padula, et al., 2017). In another study investigating dynamic properties of resting-state brain states, rather than voxel-wise BOLD variability, we found that in 22q11DS higher positive psychotic symptoms come with higher SN activation and coupling, while higher levels of anxiety are related to higher activation of the amygdala and hippocampus (Zöller et al., 2019). In these studies, we demonstrated the implication of resting-state brain dynamics in psychopathology in 22q11DS. However, which effect the brain's structural wiring has on these aberrant functional findings remains an open question.

Only two studies in 22q11DS to date have investigated structural and functional properties at the same time (Padula et al., 2015, 2017)

and none so far have attempted to examine the dynamic implications of an altered structural network architecture. Indeed, given the variety of symptoms domains and brain circuits that are affected in schizophrenia (Braun et al., 2016; Du et al., 2016; Fornito et al., 2012; Hasenkamp, James, Boshoven, & Duncan, 2011; Van Den Heuvel & Fornito, 2014) and 22q11DS (Scariati et al., 2016), we would expect abnormalities in structure and function separately, as well as alterations in structure–function relationship that cannot only be explained by the structural and functional abnormalities but are specific to their interaction. Here, we address this question by combining dynamic fMRI analysis with whole-brain tractography and principles from network control theory to investigate how the brain's white matter connectivity may influence its dynamic behavior and how this relationship is affected in patients with 22q11DS. More specifically, we extracted brain states from resting-state fMRI scans similarly to our previous study focusing on brain state dynamics (Zöller et al., 2019). Then, we calculated the control energy that is required—based on the structural connectivity of the same subjects—to persist in these specific brain states (Braun et al., 2019; Cornblath et al., 2020). Our aim was to go beyond a pure correlative

TABLE 1 Participant demographics and number of scans recorded before and after a scanner update

	HC	22q11DS	*p*-Value
Number of subjects (M/F)	78 (32/46)	77 (37/40)	.379 (χ^2)
Age mean ± *SD*	16.39 ± 5.52	17.23 ± 5.39	.342
(range)	(8.1–30.0)	(8.1–29.7)	
Right handed[a]	80.00%	77.61%	.564 (χ^2)
IQ[b]	110.80 ± 13.75	70.32 ± 12.18	<.001
Number of subjects meeting criteria for psychiatric diagnosis	*N/A*	*42 (55%)*	
Anxiety disorder	N/A	9	
Attention deficit hyperactivity	N/A	8	
Disorder (ADHD)			
Mood disorder	N/A	5	
Schizophrenia or schizoaffective disorder	N/A	3	
More than one psychiatric disorder	N/A	17	
Anxiety & ADHD & Mood & Schizophrenia		1	
Anxiety & ADHD & mood		1	
Anxiety & ADHD		11	
Anxiety & mood		3	
Anxiety & schizophrenia		1	
Number of subjects medicated	*0*	*16*	
Methylphenidate	0	9	
Anitpsychotics	0	2	
Anticonvulsants	0	1	
Antidepressants	0	1	
More than one class of medication	0	3	
Antipsychotics & antoconvulsants		1	
Antipsychotics & antidepressants		1	
Methylphenidate & antidepressants		1	
fMRI scanner type (Trio/Prisma)[c]	54/31	42/36	.209 (χ^2)
dMRI scanner type (Trio/Prisma)[c]	49/29	41/36	.227 (χ^2)

Abbreviation: N/A, not applicable.

[a]Handedness was measured using the Edinburgh laterality quotient, right handedness was defined by a score of more than 50.

[b]IQ was measured using the Wechsler Intelligence Scale for Children–III (Wechsler, 1991) for youth and the Wechsler Adult Intelligence Scale–III (Wechsler, 1997) for adults.

[c]Trio = Siemens Trio scanner (12-channel head coil, 3 T); Prisma = Siemens Prisma scanner (20-channel head coil, 3 T).

investigation of the relationship between structural and functional connectivity, and to probe the potential implications of aberrant brain structure on the brain's dynamic activation by using a mechanistic model of structure–function relationships. We take advantage of the network control theory framework to directly compare the measured temporal properties of functional brain states during resting-state fMRI, with the predicted control energy to persist in this brain state based on the structural architecture. This persistence control energy is defined as the magnitude of the required internal control input signal as predicted by the dynamic model. Through this approach, we explore whether and how the network control modeling framework could inform about disrupted structure–function relationships in psychiatric disorders.

2 | MATERIALS AND METHODS

2.1 | Participants

FMRI analyses in this study were conducted on the identical dataset as Zöller et al. (2019), which included 78 patients with 22q11DS and 85 healthy controls (HCs), aged between 8 and 30 years. For structural connectivity analysis, we used diffusion MRI (dMRI) scans acquired from the same subjects. One patient with 22q11DS and seven HCs had to be excluded from dMRI analyses because no dMRI scan was recorded for them. Table 1 shows demographic information of the remaining 77 patients with 22q11DS and 78 HCs for which both fMRI and dMRI scans were available.

Prodromal positive and negative psychotic symptoms were assessed only in patients with 22q11DS by means of the structured interview for prodromal symptoms (SIPS; Miller et al., 2003). Patients with psychiatric diagnoses are well distributed throughout the entire age range, and did not differ in their age distribution from patients without a psychiatric diagnosis (see Figure S1).

2.2 | Image acquisition

MRI scans were recorded at the Centre d'Imagerie BioMédicale (CIBM) in Geneva on a Siemens Trio (12-channel head coil) and a Siemens Prisma (20-channel head coil) 3 Tesla scanner. Table 1 contains the number of scans that were recorded before and after the update to the Prisma scanner for each image modality, respectively. There was no significant scanner-by-group interaction.

Anatomical images were acquired using a T1-weighted sequence with 192 coronal slices (volumetric resolution = $0.86 \times 0.86 \times 1.1\ mm^3$, TR = 2,500 ms, TE = 3 ms, flip angle = 8°, acquisition matrix = 256×256, field of view = 23.5 cm, slice thickness = 1.1 mm, phase encoding R >> L, no fat suppression).

FMRI scans were recorded with an 8 min resting-state session using a T2*-weighted sequence at a TR of 2.4 s (200 frames, volumetric resolution = $1.84 \times 1.84 \times 3.2\ mm^3$, TE = 30 ms, flip angle = 85°, acquisition matrix 94×128, field of view 96×128, 38 axial slices, slice thickness = 3.2 mm, phase encoding A >> P, descending sequential ordering, GRAPPA acceleration mode with factor PE = 2). Subjects were instructed to fixate on a cross on the screen, let their minds wander, and not fall asleep.

DMRI scans were acquired in 30 directions using a single shell diffusion-weighted sequence (b = 1,000 $\frac{s}{mm^2}$, one b = 0 image, volumetric resolution = $2 \times 2 \times 2\ mm^3$, TR = 8,300–8,800 ms, TE = 84 ms, flip angle = 90°–180°, acquisition matrix = 128×128, field of view = 25.6 cm, 64 axial slices, slice thickness = 2 mm, phase encoding A >> P, GRAPPA acceleration mode with factor PE = 2).

The cerebellum was not entirely captured in the resting-state scan for every individual and was thus excluded from the analysis.

2.3 | fMRI processing

2.3.1 | Preprocessing

We preprocessed fMRI scans identically as in Zöller et al. (2019) in Matlab R2017a using in-house code and functions of statistical parametric mapping (SPM12, http://www.fil.ion.ucl.ac.uk/spm/), Data Processing Assistant for Resting-State fMRI (DPARSF; Yan & Yufeng, 2010) and Individual Brain Atlases using Statistical Parametric Mapping (IBASPM; Aleman-Gomez, Melie-García, & Valdés-Hernandez, 2006). Briefly, preprocessing steps included functional realignment (registered to the mean) and spatial smoothing of fMRI frames with a Gaussian kernel of 6 mm full width half maximum, co-registration of the structural T1-weighted image to the functional mean, and segmentation of anatomical scans using the *Segmentation* algorithm in SPM12 (Ashburner & Friston, 2005). Slice-timing correction was not used as the TR is in the order of uncertainty introduced by the hemodynamic response function and to avoid interpolation of the data given the motion-sensitive nature of this dataset. The first 5 functional frames were excluded and, and cerebrospinal fluid and white matter BOLD signals were regressed out. Volumes with a framewise displacement (FD) larger than 0.5 mm were replaced with the spline interpolation of previous and following frames in order to ensure the constant sampling rate required for the retrieval of functional brain states using innovation-driven co-activation patterns (iCAPs, see following paragraph). After brain state extraction, motion frames were excluded for the computation of temporal characteristics (see below).

2.3.2 | Extracting functional brain states: Innovation-driven co-activation patterns

Following preprocessing, we extracted functional brain states from resting-state fMRI scans using the iCAPs method (Karahanoglu & Van De Ville, 2015; Zöller et al., 2018), for which code is openly available at https://c4science.ch/source/iCAPs. Briefly, steps to derive functional brain states (called "iCAPs") and their temporal properties included the hemodynamically-informed deconvolution of fMRI

timeseries using total activation (Farouj, Karahanoglu, & Van De Ville, 2017; Karahanoglu, Bayram, & Van De Ville, 2011; Karahanoglu, Caballero-Gaudes, Lazeyras, & Van De Ville, 2013). Then, significant transients were determined with a two-step thresholding procedure following Karahanoglu and Van De Ville (2015) and Zöller et al. (2018) (temporal threshold: 5–95%; spatial threshold: 5% of gray matter voxels). Subsequently, significant transient frames were spatially normalized to MNI space in order to allow clustering over all subjects. For normalization to MNI space while accounting best for anatomical variability related to age-differences and 22q11DS diagnosis, we used (DARTEL; Ashburner, 2007) on (nonsmoothed) anatomical scans to create a study-specific template, as this approach has been shown to account well for inter-subject variability (Klein et al., 2009).

Functional brain states—the iCAPs—were then determined through temporal K-means clustering on concatenated transient frames of all subjects. Brain states were computed for all subjects together in order to allow for the comparison of temporal characteristics between subjects. According to consensus clustering (Monti, Tamayo, Mesirov, & Golub, 2003), the optimum number of clusters in the present study was K = 17. Finally, a time course was estimated for each iCAP using spatio-temporal transient-informed regression with soft assignment factor ξ = 1.3 (Zöller et al., 2018). For a more detailed description of the method, we refer the interested reader to (Zöller et al., 2019), where we used the identical approach on a largely overlapping sample.

2.3.3 | Calculation of temporal activation duration and variability

The temporal activation duration of each brain state (iCAP) was computed from it's thresholded time course (z-score >|1|). We defined the activation duration as the percent of active timepoints (amplitude >|1|) with respect to the total nonmotion scanning time. To also investigate the activation range of the brain states, we additionally analyzed the activation variability, which we defined as the standard deviation of every iCAP's unthresholded time course.

2.4 | dMRI processing

DMRI scans were processed using functions from the FSL library (v5.0.11; Jenkinson, Beckmann, Behrens, Woolrich, & Smith, 2012) and from the MRtrix3 toolbox (v3.0_RC2; Tournier et al., 2019). To ensure data quality and the success of each processing step, resulting images were visually checked after every step. After denoising the dMRI scans (*dwidenoise* in MRtrix), eddy current and motion correction was conducted (*eddy_openmp* in FSL, with second level modeling, interpolation for outlier frames, and default setup otherwise). Then, the skull was stripped from eddy-corrected dMRI scans (*bet* in FSL, fractional intensity threshold = 0.3) and a white-matter mask, obtained from segmented anatomical images (using SPM12 *Segmentation* algorithm, Ashburner & Friston, 2005), was mapped to the resolution of dMRI scans (*flirt* in FSL, Jenkinson, Bannister, Brady, & Smith, 2002) and dilated by one voxel (*maskfilter* in MRtrix). Then, we estimated the single-bundle response function for spherical deconvolution based on the Tournier algorithm (Tournier, Calamante, & Connelly, 2013) and computed the fiber orientation distribution function for every voxel with a constrained spherical deconvolution (CSD; Tournier, Calamante, & Connelly, 2007). CSD-based deterministic fiber tracking (*SD_Stream* in MRtrix; Tournier, Calamante, & Connelly, 2012) was applied to reconstruct 10×10^6 streamlines longer than 10 mm. This CSD-based fiber tracking approach has the advantage that it is capable of tracking trough regions of crossing fibers, thereby overcoming limitations of more traditional tensor based approaches. To correct biological inaccuracy related to inherent bias of the stream reconstruction algorithm, spherical-deconvolution informed filtering of tractograms was performed (SIFT; Smith, Tournier, Calamante, & Connelly, 2013). In this step, the reconstructed streamlines were reduced to a number of 1×10^6 streamlines for each subject. The Brainnetome atlas (http://atlas.brainnetome.org) was warped from MNI- to subject-space using SPM12 inverse deformation created during the Segmentation step, and down-sampled to dMRI resolution (*flirt* in FSL, Jenkinson et al., 2002). Finally, a structural connectivity matrix $\mathbf{A} \in \mathbb{R}^{N_{reg} \times N_{reg}}$ was reconstructed for every subject by counting the streamlines connecting each of the N_{reg} = 234 regions in the Brainnetome atlas. Main analyses were conducted on the non-normalized streamline count matrices, and replicated on normalized structural connectivity, where streamline counts were divided by the joint relative volume of the connected regions (see Figure S6). This joint relative volume was defined as the total number of voxels covered by both regions divided by the total number of brain voxels in the Brainnetome atlas in subject space.

2.5 | Minimum control energy to persist in a brain state

In this study, we used linear control theory for brain network analysis, an approach that uses principles from control and dynamical systems theory to investigate the impact that the brain's structural topology may have on its functional dynamics (Kim & Bassett, 2019; Lynn & Bassett, 2019; Tang & Bassett, 2018). Under the assumption of a linear model of dynamics (Kim & Bassett, 2019), and control from all regions of the brain, we estimated the minimum control energy required to persist in specific brain states. For extended reviews on the control of brain network dynamics, we refer the interested reader to (Lynn & Bassett, 2019; Tang & Bassett, 2018). In the following paragraphs, we describe the linear dynamic model used here, and outline the mathematical basis for the computation of the minimum control energy based on this model, as well as the way in which brain states of interest were defined in order to estimate persistence control energy. The computation of persistence control energy was done using in-house Matlab code that was based on the functions published with (Cornblath et al., 2020).

2.5.1 | Dynamic model

In order to study how the white-matter anatomy of the brain constrains or facilitates state transitions, we modeled the brain as a continuous linear time-invariant dynamic system following Gu et al. (2017) and Betzel et al. (2016)

$$\dot{\mathbf{x}}(t) = \mathbf{A}_s\mathbf{x}(t) + \mathbf{B}\mathbf{u}(t),$$

in which $\mathbf{x}(t) = \left[x_1(t),\ldots,x_{N_{\text{reg}}}(t)\right]^\top \in \mathbb{R}^{N_{\text{reg}}\times 1}$ is the brain's functional state at timepoint t given by the activity level $x_i(t)$ in each region i, and $\dot{\mathbf{x}}(t)$ is the time derivative of $\mathbf{x}(t)$. The dynamic behavior of the brain is constrained by the stabilized structural white matter connectivity matrix $\mathbf{A}_s$, which is derived from the original structural connectivity matrix $\mathbf{A}$, where each element A_{ij} is the number of streamlines connecting regions i and j. In order to ensure stability of the dynamic system, all eigenvalues of $\mathbf{A}_s$ have to be below 0. Therefore, we stabilized the system by dividing the original structural connectivity matrix $\mathbf{A}$ by its largest eigenvalue $\lambda_{\max}$ and subtract the identity matrix $\mathbf{I}$: $\mathbf{A}_s = \frac{\mathbf{A}}{\|\lambda_{\max}\|+1} - \mathbf{I}$ (Betzel et al., 2016). The diagonal matrix $\mathbf{B}\in\mathbb{R}^{N_{\text{reg}}\times N_{\text{reg}}}$ specifies the set of control nodes. Throughout this study, we assume that all regions of the brain can be controlled and therefore $\mathbf{B} = \mathbf{I}$. Finally, $\mathbf{u}(t) = \left[u_1(t),\ldots,u_{N_{\text{reg}}}(t)\right]^\top \in \mathbb{R}^{N_{\text{reg}}\times 1}$ contains the control input signals $u_i(t)$ at region i and timepoint t.

Notably, the comparison of different graph models shows that there are marked differences in controllability across different types of networks, indicating that characteristics of brain network controllability are unique and potentially relevant for cognitive function (Wu-Yan et al., 2018).

2.5.2 | Persistence control energy

In this study, we wished to investigate the structural control energy that is necessary to persist in a certain brain state $\mathbf{x}$ for a duration T. Throughout this study, we compute control energy for a control horizon of $T = 1$ (Betzel et al., 2016). The optimum control input $\mathbf{u}_{\min}$ associated with minimum control energy can be found by solving (Antsaklis & Michel, 2005)

$$\mathbf{u}^* = \min_{\mathbf{u}} E_{\min} = \min_{\mathbf{u}} \int_{t=0}^{T} \mathbf{u}(t)^T\mathbf{u}(t)dt.$$

The analytical solution of this minimization problem is given by the minimum energy

$$E_{\min} = \left(\mathbf{x}(T) - e^{\mathbf{A}T}\mathbf{x}(0)\right)^\top \mathbf{W}_r^{-1}(T)\left(\mathbf{x}(T) - e^{\mathbf{A}T}\mathbf{x}(0)\right),$$

with the *reachability Gramian*

$$\mathbf{W}_r(T) = \int_{t=0}^{T} e^{\mathbf{A}(T-t)}\mathbf{B}\mathbf{B}^\top e^{\mathbf{A}^\top(T-t)}dt.$$

The optimal control input with this minimum energy can be explicitly computed for each timepoint t:

$$\mathbf{u}^*(t) = \mathbf{B}^\top e^{\mathbf{A}^\top(T-t)}\mathbf{W}_r^{-1}(T)\left(\mathbf{x}(T) - e^{\mathbf{A}T}\mathbf{x}(0)\right).$$

The required control energy at every brain region is given by $E_i = \int_0^T \left\|u_i^*(t)\right\|^2 dt$ and the total control energy can be computed by summing over all regions $E = \sum_{i=1}^{N_{\text{reg}}} E_i$.

Throughout this manuscript, we investigated persistence control energy, that is, the minimum control energy in the case where initial and target states are identical: $\mathbf{x}(0) = \mathbf{x}(T) = \mathbf{x}$. Then, minimum persistence control energy E_P is defined by

$$E_P = \sum_{i=1}^{N_{\text{reg}}} E_{Pi} = \sum_{i=1}^{N_{\text{reg}}} \int_0^T \left\|u_{Pi}^*(t)\right\|^2 dt,$$

with

$$\mathbf{u}_P^*(t) = \mathbf{B}^\top e^{\mathbf{A}^\top(T-t)}\mathbf{W}_r^{-1}(T)\left(\mathbf{x} - e^{\mathbf{A}T}\mathbf{x}\right).$$

2.5.3 | Definition of brain states

Persistence control energy E_P as defined above was computed for every iCAP k. As iCAP maps are originally voxelwise without any parcellation (see Section 2.3), the maps were atlased by averaging the values of the z-scored spatial map across the voxels of each of the 234 brain regions of the Brainnetome atlas. This procedure resulted in the brain state vectors $\mathbf{x}_k(0) = \mathbf{x}_k(T) = \mathbf{x}_k$ that correspond to the atlased iCAP maps containing the average iCAP values in each region. In order to minimize noise susceptibility, we thresholded the brain states at a z-score of 1.5; in other words, regions with an average z-score <1.5 were set to zero.

2.5.4 | Weighted degree of brain states

In order to compare persistence control energy to overall structural connectivity strength of each brain state, we defined the structural connectivity strength $d_{iCAP,k}$ of a brain state k as the weighted sum of this regional weighted degree d_n, multiplied by the spatial map $\mathbf{x}_k$ of each brain state:

$$d_{iCAP,k} = \sum_{n=1}^{N_reg} d_n * x_{k,n},$$

with N_{reg} the number of brain regions, d_n the degree of the region (sum of edge weights connecting to that region), and $x_{k,n}$ the value iCAP k in region n.

2.6 | Statistical analysis

2.6.1 | Group comparisons of duration and persistence control energy

Two-sample *t*-tests were used to compare functional and structural measures between patients with 22q11DS and HCs. Permutation testing based on maximum T-statistics (Westfall & Young, 1993) using 5,000 permutations was used to correct for multiple comparisons.

2.6.2 | Partial least squares correlation: Multivariate relationship between brain measures and age

We used partial least squares correlation (PLSC; Krishnan, Williams, McIntosh, & Abdi, 2011) to retrieve patterns of age-relationship in persistence control energy of all iCAPs. The steps of PLSC include

1. Computation of concatenated group-wise correlation matrices $\mathbf{R} = \begin{bmatrix} \mathbf{R}_{HC} \\ \mathbf{R}_{22q} \end{bmatrix} = \begin{bmatrix} \mathbf{Y}_{HC}^{\top}\mathbf{X}_{HC} \\ \mathbf{Y}_{22q}^{\top}\mathbf{X}_{22q} \end{bmatrix}$ between age in $\mathbf{Y} \in 1 \times N_{sub}$ and persistence control energy in $\mathbf{X} \in K \times N_{sub}$ of each brain state $k = 1, \ldots, K$ and subject $s = 1, \ldots, N_{sub}$. $\mathbf{Y}_{HC}$, $\mathbf{Y}_{22q}$, $\mathbf{X}_{HC}$, and $\mathbf{X}_{22q}$ are *z*-scored across subjects.
2. Singular value decomposition of $\mathbf{R} = \mathbf{USV}^{\top}$ to obtain a number of correlation components (also often called "latent variables"). Singular values on the diagonal of **S** indicate the explained correlation by each component. Every component is associated with one age weight per group (also often called "age saliences") in **U** that indicate how strong the age relationship is present in each group, as well as with one brain weight per brain state (also often called "brain saliences") in **V** that indicate how strongly each brain state contributes to the multivariate correlation between age and persistence control energy. These age weights and corresponding brain weights indicate the effect strength in each brain state. Because **X** and **Y** were *z*-scored in the first step, **R** corresponds to a correlation matrix, and as a consequence the age weights and brain weights can be interpreted similar to correlation values.
3. Permutation testing with 1,000 permutations to test for significance of correlation components, where rows of **X** were randomly permuted, while leaving **Y** unchanged, in order to estimate the null distribution of singular values **S** under assumption of no significant correlation between **Y** and **X**.
4. Bootstrapping with 500 bootstrap samples, obtained through sampling with replacement the observations in **Y** and **X**, to evaluate the stability of age- and brain weights in a significant correlation component.

Altogether, PLSC allows to retrieve components that summarize the multivariate correlation between a number of behavioral measures and a number of brain measures. Each significant correlation component contains "behavior weights" (here: age weights) and "brain weights" (here: "persistence control energy weights") that indicate, which behavior is most strongly correlated with which brain measure. For a more detailed description of PLSC, we refer the interested reader to (Krishnan et al., 2011; Zöller, Padula, et al., 2017; Zöller, Schaer, et al., 2017; Zöller et al., 2018).

2.6.3 | Nuisance variable regression

Age, sex and full-scale intelligence quotient (FSIQ) were included as nuisance regressors in group comparisons and only sex was used in age-PLSC analyses. Nuisance regressors were standardized within each group to avoid insensitivity to group differences introduced by systematic group differences, especially in FSIQ.

2.7 | Relationship between brain state function and structure

In order to assess the relationship between resting-state fMRI activation measures and persistence control energy, we compute Pearson correlations between the two measures. First, we computed correlations across subjects for each group and each brain state, resulting in $K = 17$ correlation values per group. We then compared these 17 values between HCs and patients with 22q11DS using a paired *t*-test. Second, we computed correlations across the $K = 17$ brain states for each subject. We then compared the correlation values between HCs and patients with 22q11DS using a two-sample *t*-test.

3 | RESULTS

3.1 | Spatial and temporal properties of resting-state functional states

Using iCAPs, we extracted 17 functional brain states from the resting-state fMRI scans. The optimal number of states was determined using consensus clustering (Monti et al., 2003). Extracted networks include well-known resting-state brain states, such as DMN, FPN, and SN states (see Figure S2). Patients with 22q11DS have significantly altered activation duration in five brain states, including both brain states with longer activation duration, and brain states with shorter activation duration (see Figure S3). For a detailed discussion of temporal properties and their relevance for clinical symptoms in 22q11DS, we refer the interested reader to (Zöller et al., 2019).

3.2 | Persistence control energy in brain networks is lower than in random networks

We computed persistence control energy of the 17 brain states for every participant based on his or her individual structural connectivity

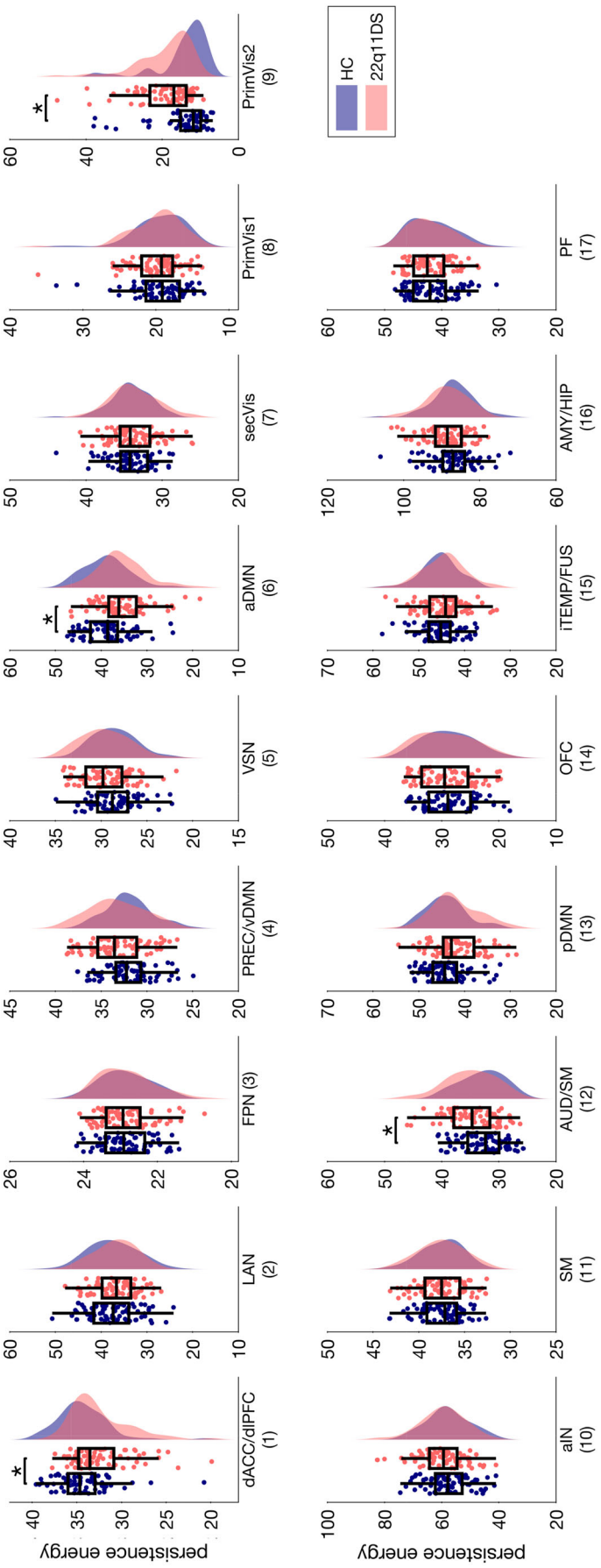

FIGURE 1 Group differences in persistence control energy of the 17 functional brain states in patients with 22q11DS compared to HCs. *p*-values are corrected for multiple comparisons based on permutation testing (Westfall & Young, 1993); age, sex and FSIQ were included as covariates. Significant group differences ($p < .05$) are marked with an asterisk. Single-subject duration measures are included as scatterplots. All *p*-values and *T*-statistices can be found in Table S1. aDMN, anterior DMN; aIN, anterior insula; AMY/HIP, amygdala/hippocampus; AUD/SM, auditory/sensorimotor; dACC/dlPFC, dorsal anterior cingulate cortex/dorsolateral prefrontal cortex; FPN, fronto-parietal network; iTEMP/FUS, inferior temporal/fusiform; LAN, language network; OFC, orbitofrontal cortex; pDMN, posterior DMN; PFC, prefrontal cortex; PREC/vDMN, precuneus/ventralDMN; PrimVIS1, primary visual 1; PrimVIS2, primary visual 2; SecVIS, secondary visual; SM, sensorimotor; VSN, visuospatial network

matrix. In order to verify whether the persistence control energy values that we measure for human brain networks are different from random networks, we computed for every brain state the persistence control energy based on 100 random null networks that preserve the structural network topology created from every subject's structural connectivity matrix (Rubinov & Sporns, 2010). The spatial distribution of brain state maps were kept intact. For all states, the energy for these random networks was significantly higher than for the true brain networks (see Figure S4), confirming previous findings by Cornblath et al., 2020 who also observed that brain networks are specifically wired to reduce control energy.

To furthermore test how specific the energy is to the particular data-driven resting-state brain states, we computed the persistence control energy for 100 brain states, in which regional brain state activation (i.e., atlased iCAPs activation as described in the methods, Section 2.5) was randomly shuffled between regions. Structural connectomes were kept intact for this test. For all states, the persistence control energy for randomly shuffled states was significantly higher than for the true brain state (see Figure S5), indicating that the spatial distribution of functional brain states reduces persistence control energy given the brain's structural topology.

3.3 | Persistence control energy of functional brain states is altered in patients with 22q11DS

Aberrant structural connectivity in patients with 22q11DS leads to altered persistence control energy in four out of the 17 brain states (see Figure 1). Persistence control energy was higher in patients with 22q11DS in brain states that involve more posterior and dorsal regions—primary visual 2 (PrimVIS2) and auditory/sensorimotor (AUD/SM). Reductions of persistence control energy on the other hand were present mainly in brain states including more anterior regions—dorsal anterior cingulate cortex/dorsolateral prefrontal cortex (dACC/dlPFC) and anterior DMN (aDMN). For structural connectivity controlled for region size, the pattern of group differences in persistence control energy resembles those for non-normalized structural connectivity (see Figure S6a).

3.4 | Structural connectivity (weighted degree) alterations are inversely related to persistence control energy alterations

As we investigate persistence control energy allowing all brain regions to be controlled, and using a linear dynamic model, we expect persistence control energy to be closely related to the weighted degree of the brain regions in each brain state (Karrer et al., 2020). The specific relationship between structural connectivity and controllability varies for different controllability measures, such as for example average controllability, modal controllability, or minimum control energy, and further depends on the model that is used (Karrer et al., 2020). Therefore, and to investigate this aspect in more depth, we calculated the structural connectivity weighted degree $d_{iCAP,k}$ of each brain state k and compared this measure between groups using univariate t-tests (see Figure S7). The results show significant group differences between patients with 22q11DS and HC subjects in three brain states that all have also significantly altered persistence control energy (higher in dACC/dlPFC and aDMN, and lower in PrimVis2). These results indicate that reduced persistence control energy in patients with 22q11DS is related to higher structural connectivity of the corresponding brain states, whereas higher persistence control energy in other brain states is accompanied by weaker structural connectivity of these states.

3.5 | Persistence control energy decreases from childhood to adulthood

There is one significant correlation component (p <.001) resulting from PLSC analysis testing for a relationship between persistence control energy and age (see Figure 2). Persistence control energy is negatively correlated with age in 7 out of the 17 states, as reflected by negative iCAPs persistence control energy weights (Figure 2b). This correlation with age is significant for both groups (Figure 2a). Brain states that show a stable relationship between persistence control energy and age include anterior and posterior DMN, anterior insula (aIN), sensory states (primary visual 1 (PrimVIS1) and sensorimotor (SM)), one emotional state (AMY/HIP), and the language state. The persistence control energy of states that are commonly associated with goal-directed behavior during tasks do not show any relationship with age (i.e., precuneus/ventral DMN (PREC/vDMN), which is sometimes called dorsal attention state, FPN, and visuospatial network (VSN)).

3.6 | No correlation across subjects between activation duration and persistence control energy

In order to test whether there was a relationship between structural and functional measures across subjects, we computed correlations between resting-state activation duration and persistence control energy across subjects for each state. In a comparison of group differences in persistence control energy (Figure 1) and group differences in resting-state activation (Figure S3), no clear pattern of common alterations emerged (see Figure S8). Therefore, we expected no linear correspondence between the two measures. Indeed, there was no significant correlation between the two measures either in patients with 22q11DS or in HCs (see Figure 3a). In other words, a subject who spent a long time in one brain state during the resting-state fMRI scan (measured through iCAPs activation duration), did not have a systematically higher or lower persistence control energy (based on the subject's structural connectivity and a model of brain dynamics) of that brain state compared to other subjects.

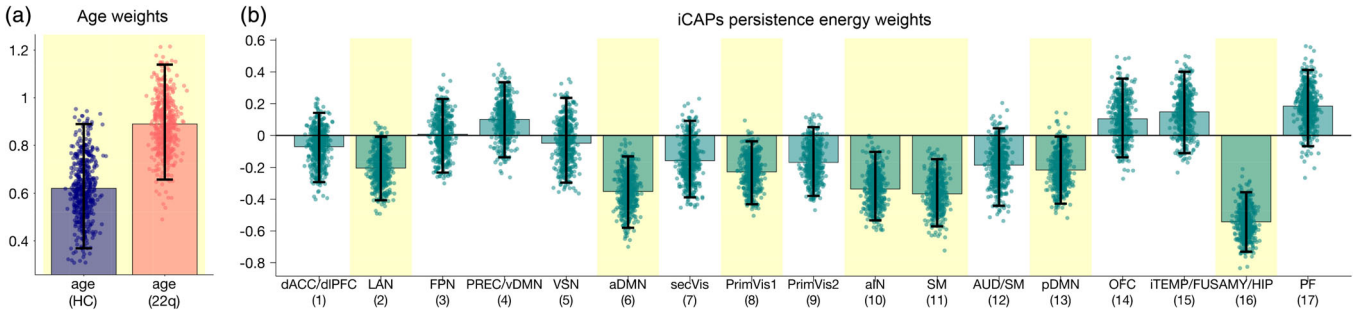

FIGURE 2 PLSC testing for a relationship between persistence control energy and age resulted in one significant correlation component (p <.001). (a) According to age weights indicating the correlation strength in each group, the age-relationship is stable in both groups (confidence intervals not crossing zero). (b) Persistence control energy weights show that there is a stable negative relationship with age in 7 out of the 17 brain states. Error bars indicate bootstrapping 95% confidence intervals; stable results were indicated by yellow background. Sex was included as nuisance regressor in the analysis. Mean and percentile values of bootstrap distributions can be found in Table S2

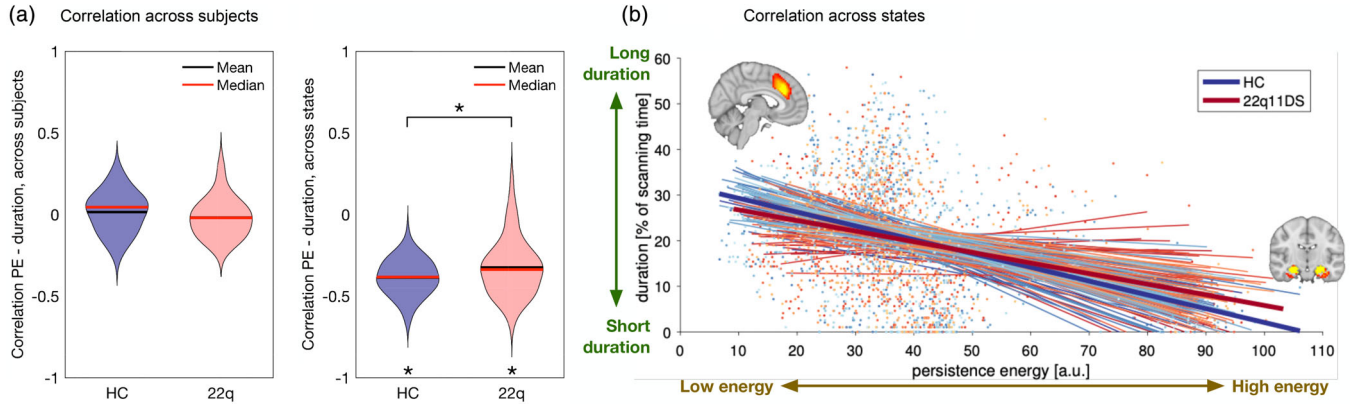

FIGURE 3 Correlation between persistence control energy and resting-state activation duration. (a) Across subjects there is no significant correlation, either in patients with 22q11DS or in HCs. Violin plots show the distribution of correlations for all brain states. p = .434, T = −0.80. (b) Across states there is a negative correlation between the two modalities: the higher the persistence control energy, the shorter the resting-state activation duration. This correlation is significantly stronger in HCs than in patients with 22q11DS. Left: Violin plots show the distribution of correlations for all subjects. Significant group differences (p <.05) are marked with an asterisk. p = .013, T = 2.50. Right: every line corresponds to the fitted linear curve for each subject, thick lines show the average correlation of each group. PE, persistence control energy

3.7 | Negative correlation across states between activation duration and persistence control energy

To test whether within each subject there was a relationship between temporal activation and persistence control energy, we computed across-states correlations for each subject (see Figure 3b). There was indeed a negative correlation between activation duration and persistence control energy. In other words, all subjects tend to spend less time in brain states whose structural wiring leads to higher persistence control energy. This negative correlation was significantly stronger (lower) in HCs than in patients with 22q11DS (p = .010).

To test whether this correlation between structure and function changes over age, we tested for a relationship with age of these negative correlation values (see Figure 4). In HCs, the energy-activation correlation did not change over age (c = −.03, p = .937). In patients with 22q11DS, however, the correlation became significantly weaker (higher negative values) with increasing age (c = .37, p = .005). In a joint model, the group-by-age interaction was significant with p = .002. In other words, while at a younger age, patients showed similar energy-activation relationship as HCs, older patients have a weaker negative energy-activation correlation, indicating that the observed weakening in correlation (see previous paragraph) is emerging over age.

There was no correlation with FSIQ (HCs: c = .08, p = .728; 22q11DS: c = −.01, p = .0.937), positive psychotic symptoms as measured by the sum of positive SIPS scores (22q11DS: c = −.12, p = .688) and negative psychotic symptoms as measured by the sum of negative SIPS scores (22q11DS: c = −.37, p = .130). In FSIQ and SIPS analyses, age and sex were included as nuisance regressors, reported p-values were corrected for the six computed correlations (age and FSIQ in both groups, positive and negative SIPS in patients) using the false discovery rate.

3.8 | Activation variability is similarly related to persistence control energy as activation duration

In order to investigate the relationship of persistence control energy with the activation range of activation during rest, we repeated the

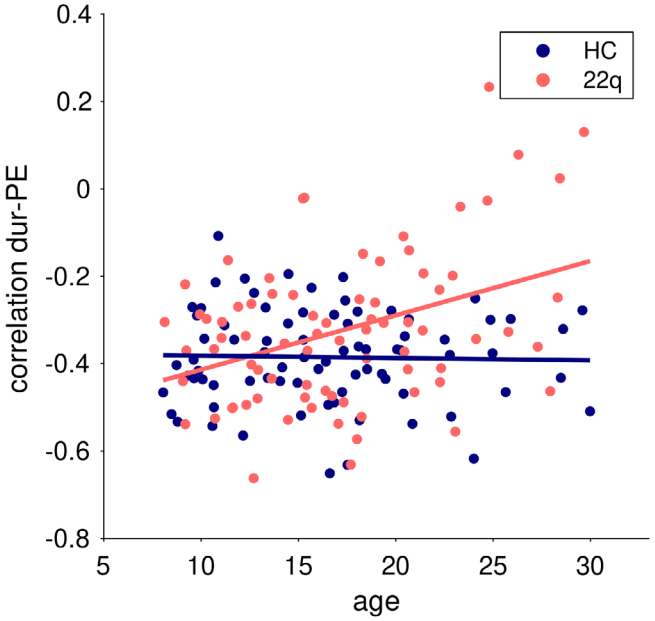

FIGURE 4 The negative correlation between persistence control energy and activation duration across brain states is constant over age in HCs (c = −.03, p = .937), but significantly increasing (i.e., weakening) with higher age in patients with 22q11DS (c = .38, p = .005). Sex was included as nuisance regressor. Dur, activation duration; PE, persistence control energy

analyses using activation variability (i.e., the standard deviation) instead of activation duration of each brain state (see Figure S9). Interestingly, variability group differences strongly resemble group differences in activation duration, which suggests that higher duration comes along with larger deviation from the mean activity. Further, when correlating persistence control energy with time course variability, we confirm the finding of a weakened across-states correlation in patients with 22q11DS that is also more pronounced in older patients.

4 | DISCUSSION

In this study, we used dynamic models based on network control theory to investigate the link between aberrant structural connectivity and the activation of functional brain states during rest. We investigated whether the relationship between structure and function is altered in patients with 22q11DS, a population at extremely high risk for schizophrenia. Our overall goal was to test whether such an alterations could give insights on possible mechanistic implications of aberrant brain structure on altered functional activation (Braun et al., 2018).

To address this question, we retrieved functional brain states and their activation duration from resting-state fMRI scans. Then, we used network control theory to predict the control energy that would be necessary to persist in these functional states based on structural connectivity measured in diffusion MRI (Braun et al., 2019; Cornblath et al., 2020). Finally, we investigated the relationship between the temporal activation during rest and this predicted persistence control energy, in order to estimate how the brain's white matter anatomy may be linked to the activation behavior of functional brain states. As this is one of the first studies using network control theory to investigate a clinical population, our aim was to explore whether and how this approach could give insights into aberrant structure–function relationships in psychiatric disorders that would not be captured by alterations in one single modality on its own.

We found aberrant persistence control energy of several brain states, mainly involving anterior or posterior medial connections. Further, persistence control energy decreased from childhood to adulthood in 7 out of 17 brain states both in patients with 22q11DS and HCs. Finally, when probing for a relationship between structural persistence control energy and functional resting-state activation, we found a negative correlation across brain states consistent with prior work (Cornblath et al., 2020), which was less pronounced in patients with 22q11DS. However, even though in some brain states both persistence control energy and functional activation were altered in patients with 22q11DS, we found no systematic relationship between persistence control energy of a brain state and its functional activation across subjects. In the following exposition, we will first discuss the alterations of persistence control energy and altered structure–function relationships in patients with 22q11DS, and then offer a tentative explanation for the absence of an across-subject relationship between control energy and functional activation.

4.1 | The architecture of human structural brain networks and functional brain states support low persistence control energy

Overall, we confirmed previous findings comparing persistence control energy in human brain networks with those of randomized networks (Cornblath et al., 2020). For both patients with 22q11DS and HCs, persistence control energy was lower in real brain networks than in topology-preserving random networks. Also, when keeping structural connectomes intact, persistence control energy for the true data-driven brain states was lower than for spatially shuffled brain states. Together, these results indicate that both human structural white matter topology, and functional brain state architecture, support the engagement in brain states at low energetic cost.

4.2 | Anterior–posterior and medial-lateral gradient of altered connectivity leads to aberrant brain control energy in 22q11DS

The first goal of this study was to investigate persistence control energy of data-driven resting-state functional brain states in patients with 22q11DS. We found that aberrant structural wiring leads to a pattern of altered control properties with some brain states requiring higher persistence control energy and others requiring lower

persistence control energy. Persistence control energy is mainly reduced in frontal brain states (aDMN, dACC/dlPFC) and increased in occipital (PrimVIS2) and lateral parietal (AUD/SM) brain states. These alterations were inversely related to altered weighted degree, for which frontal brain states (aDMN, dACC/dlPFC) showed increases, whereas the occipital PrimVIS2 brain state showed reductions. This pattern of findings confirms prior reports of aberrant anterior–posterior and medial-lateral white-matter connectivity in patients with 22q11DS, which was found to relate to positive and negative psychotic symptoms (Gothelf et al., 2011; Scariati et al., 2016; Váša et al., 2016). Our study expands upon these prior studies by probing the impact of this aberrant wiring on the activation behavior of the brain in terms of the predicted persistence control energy that is needed to engage in these brain states. Profound reductions of persistence control energy were present in DMN and cingulo-frontal SN, which are two brain systems that are known to play a central role in higher order cognition (Menon, 2011). Previous reports provide evidence that the structural and functional connectivity of these brain states is altered in patients with 22q11DS (Padula et al., 2015; Padula, Schaer, et al., 2017; Schreiner et al., 2014). In particular the dACC, which is a central node of the SN, has been found to be affected in 22q11DS using different neuroimaging modalities and alterations of this brain region have been suggested as a biomarker for psychosis in the disorder (Padula, Scariati, Schaer, & Eliez, 2018). Lower persistence control energy in these brain states in patients with 22q11DS may seem counterintuitive, as the healthy brain is assumed to decrement energy. Speculatively, the effect could be related to compensatory effects in less symptomatic patients. However, patients with 22q11DS do not spend more time in these energetically more advantageous states, so even though these brain states should be more easily accessible, they do not make use of this advantage. Further research on the relationship between persistence control energy and different clinical profiles of individuals with 22q11DS would be promising to investigate this effect in more detail.

4.3 | Persistence control energy gets lower from childhood to adulthood

Aside from alterations in 22q11DS, we found that persistence control energy of many brain states (7 out of 17) is negatively correlated with age, both in patients with 22q11DS and in HCs. This finding suggests that with increasing age, the brain gets increasingly well wired to reduce the control energy required for its functional activation. In line with these findings, Tang et al. found that both average and modal controllability (which measure the general ability to steer the brain toward easy-to-reach or difficult-to-reach brain states) increase over age in a similar age range, which suggests an increasingly economical wiring that at the same time allows a higher diversity of brain dynamics (Tang et al., 2017). Importantly, while there are small variations in the distributions of controllability across the brain in males and females, the trend for increasing controllability with age is equally strong in both sexes (Cornblath et al., 2018). Further, Cui et al. (2020) found that control energy of atlas-based brain states calculated with a comparable approach to ours, was also decreasing from childhood to adulthood in most brain states (Cui et al., 2020). This developmental trajectory of structural brain architecture was preserved in patients with 22q11DS, suggesting that while they present with absolute alterations of controllability properties, their overall development seems to be largely intact.

4.4 | Higher use of persistence control energy in patients with 22q11DS, which becomes increasingly marked with age

When investigating the relationship between functional activation and structural persistence control energy, we found that the brain activates in a highly cost-effective way, spending less time in brain states that are energetically more demanding, consistent with prior evidence in a completely different cohort (Cornblath et al., 2020). Interestingly, this relationship was similar for activation variance, suggesting that shorter activation duration comes along with a lower activation range during rest. In patients with 22q11DS, this negative relationship was significantly weaker than in HCs, which suggests that aside from the pure alteration in structure and function, the relationship between the two is also altered. In particular, patients use their brains in a less energy-preserving way, spending more time in energetically demanding states than HCs. Additionally, this higher energetic cost of functional activation in patients with 22q11DS became increasingly marked with greater age, indicated by a weaker negative correlation between persistence energy and activation duration in patients at higher age. Possibly, the patients' energetically more costly use of their brain may express in the more severe symptomatology characteristic of older patients. Divergent trajectories during adolescence have for instance been reported for executive functions (Maeder et al., 2016). However, here we did not find a significant correlation between our measure of functional use of energy and psychotic symptoms or FSIQ. The absence of such behavioral relationships could indicate that this measure of functional use of energy is not directly related to the presence of psychotic symptoms or cognitive impairment. Instead, the developmental failure to optimize brain function to the underlying structural wiring could represent a global property of brain function in 22q11DS. Of note, excluding the five patients with a diagnosis of schizophrenia from the analysis did not alter the overall results (see Figures S10 and S11), further supporting this notion that the observed alterations represent a general trend of brain alterations in 22q11DS. The observed ineffectiveness in decrementing energy through functional activation could potentially contribute to a broad vulnerability for psychopathology. Specific aspects of the psychiatric phenotype (i.e., anxiety of psychotic symptoms) might then develop as a consequence of alterations in functional activity rather that the specific wiring of individual networks. To confirm this hypothesis, longitudinal studies will be required along with replication in other populations carrying vulnerability to psychopathology other that 22q11DS, such as for instance in

individuals with Clinical-High-Risk for Psychosis (Fusar-Poli et al., 2013). Additionally, future studies with larger sample sizes, and targeting more specific measures of particular clinical symptoms and executive functions, would be required to draw a final conclusion on this effect.

4.5 | Control energy and activation alterations manifest in similar brain states, but are not systematically correlated across subjects

While we were able to detect a relationship between functional activation duration and structural persistence control energy across states (pointing toward the inherently cost-effective activation of the human brain as discussed above), we did not observe a relationship across subjects. In other words, subjects with energetically less advantageously wired brain states (higher persistence control energy) did not systematically spend more or less time in these brain states compared to other subjects. This can also be seen when comparing the alterations that we find in persistence control energy with results from our previous study, where we investigated functional properties in the identical subjects by also using the iCAPs approach to assess temporally overlapping brain state activation (Zöller et al., 2019). As indicated by the absence of across-subject correlations (Figure 3a), the direction of alterations of resting-state activation duration obtained in that study was not linearly related to structural persistence control energy alterations found in the present study. This suggests that the measure of iCAPs activation duration, and persistence control energy represent different types of brain alterations in these patients. However, there were overlapping results in some of the brain states (dACC/dlPFC and aDMN, see Figure S8), which indicates that in these particular brain states, both structural and functional properties play a role in the 22q11DS symptomatology.

In particular, in this previous study we found a relationship between altered resting-state activation in DMN and cingulo-frontal SN and higher levels of anxiety (anterior DMN), and positive psychotic symptoms (cingulo-frontal SN; Zöller et al., 2019). Furthermore, and in line with the literature on the role of the amygdala and hippocampus in anxiety (Etkin & Wager, 2007), we found that higher functional activation duration and aberrant functional coupling of the amygdala and hippocampus brain state tracks with higher levels of anxiety. In the present study, we confirm that DMN and cingulo-frontal SN are also affected in terms of structural connectivity measured through diffusion MRI, and that this alteration in structural wiring leads to aberrant controllability properties in patients with 22q11DS. Future studies should examine whether these alterations are also linked to higher levels of anxiety and the risk for developing psychosis as suggested by our previous functional and anatomical findings (Mancini et al., 2019; Zöller et al., 2019).

Importantly, brain states do not act in isolation, but interact among themselves. For instance, knowing about the interaction between the DMN and the amygdala and hippocampus that we discovered in the same dataset (Zöller et al., 2019), one could imagine that indeed alterations of controllability in the DMN may lead to increased activity of the amygdala and hippocampus. Testing for such cross-network relationships may be even more interesting, and our methodological approach offers a valuable framework to explore this complexity in future research.

4.6 | Significance and implication for the pathophysiology in schizophrenia

Altogether, the results presented here show that network control theory, and in particular persistence control energy, can provide insights into global structure–function relationship of the human brain. Through the assumption of a dynamic model of brain function, it allowed us to go beyond a pure description of structure–function relationship in specific brain states, and provide a prediction of the effect that altered structural wiring has on the brain's functional activation in terms of energy cost. Our results suggest that a negative relationship between functional activation and energy cost across brain states is global property of the brain's function in every individual. The overall reduction of this relationship in a population at risk for schizophrenia suggests that psychiatric disease affects the brain in a way that makes it's functional activation more energetically costly. However, this relationship did not relate to clinical variables, which could mean that this property represents a trait marker of vulnerability to psychopathology rather than a state marker related to the presence of symptoms at the time of scanning. A recent study investigating network control energy in patients with schizophrenia using a very similar approach to the one used here found increased control energy in a task-related working-memory brain state in patients with schizophrenia (Braun et al., 2019). These results also point toward an energetically more demanding structural wiring of the brain in patients with schizophrenia. Together with the dysfunctional activation of structurally affected brain states that we find here, these results provide an interesting starting point for future analyses of brain structure and function in schizophrenia, and psychiatric diseases in general. Of note, our results support the view that brain structure and function are not only affected independently, but that psychiatric disease comes also with alterations in their interrelationship, which cannot only be explained by structural and functional abnormalities. An investigation of larger samples, and possibly also task-fMRI data, would be promising to confirm the findings of this study, and get further insights into this aberrant relationship between functional activation and structural architecture.

4.7 | Methodological considerations and limitations

4.7.1 | Placement among existing state-of-the-art control strategies

The approaches using control theory to analyze brain networks can be differentiated based on the control strategies they use. Initial studies

on controllability of brain networks examined properties like average and modal controllability, which assess the ease of a local or distant state transition while ignoring the nature of either the initial or target states (e.g., Gu et al., 2015; Jeganathan et al., 2018; Tang et al., 2017). Studies on specific state trajectories, on the other hand, stipulate the initial and target states and assess the energy necessary for that specific trajectory (Betzel et al., 2016; Cui et al., 2020; Gu et al., 2017). In this case, states could be defined either by activating all regions in a cognitive system defined from the literature (Betzel et al., 2016; Cui et al., 2020; Gu et al., 2017), or by choosing a data-derived brain state (Braun et al., 2019; Cornblath et al., 2020). Similar to the latter two studies (Braun et al., 2019; Cornblath et al., 2020), here we investigated the energy to persist in specific states, and we defined the brain states in a data-driven way from fMRI data acquired from the same subjects. Using this approach, we found profound differences in control energy of multiple states in patients with 22q11DS. These findings underline the potential of data-driven brain states to detect relevant subject-specific alterations, which is promising for future studies involving other clinical populations.

Of note, while in the present study we focused on the characterization of individual brain states and thus solely investigated persistence control energy of single brain states, the control energy framework also allows to estimate the required energy to transition between different brain states (Braun et al., 2019; Cornblath et al., 2020). The analysis of the relationship between such transition control energy and the functional co-activation between different brain states (Zöller et al., 2019) would be an interesting future avenue following up on this study.

4.7.2 | Different scales of brain network dynamics

Importantly, there are different types of brain network dynamics. On one hand, functional activation of pathways entails neural plasticity and changes the structural connections (Bassett et al., 2018). At the same time, functional activation is constrained by the anatomy that it happens on. In this study, we used network control theory to investigate the latter effect by modeling the energetic cost of dynamic activation that happens on top of a fixed anatomical network. The question of changes in structural connectivity was not addressed in this study, and different approaches and data would be required to model such dynamics of the anatomical networks themselves (Bassett et al., 2018). Going even further and integrate both dynamics on and of the network together in more complex models would be a promising direction for future analyses to obtain a more complete picture (Bassett & Sporns, 2017).

4.7.3 | Variance of structural connectivity across subjects and across regions has different scales

In the present study, structural connectivity was measured in terms of connection density; that is, with a fixed number of reconstructed streamlines. As a result, the variability of connectivity across regions is relatively high compared to the variability across subjects. Therefore, this approach supports a careful investigation into *relative* changes in connectivity, but it is less powerful in tracking *absolute* changes in connectivity. In our results, this effect can be observed in Figure 1, where the differences in energy from one state to another are much larger than the differences in persistence control energy across subjects for one single brain state. Significant differences between subjects do exist, however, they are small with respect to the differences between brain states. This effect may be a possible reason why we detected correlations with functional activation across brain states, but not across subjects.

4.7.4 | Linear models of brain dynamics

For simplicity, here we chose to use a linear model of dynamics on the structural connectivity graph (Gu et al., 2015; Honey et al., 2009; Kim & Bassett, 2019) to calculate minimum control energy (Betzel et al., 2016). Even though this model is the most widely used approach for network control theory in neuroscience, it may be overly simplistic. Incorporating models of nonlinear dynamics could prove useful in the future as they could potentially improve the estimation of more realistic control energy (Kim & Bassett, 2019). It is possible that an estimate based on more biologically plausible dynamic models would allow us to detect more subtle relationships between controllability and functional activation.

4.7.5 | Relevance for other imaging modalities

While the results presented here were obtained for fMRI brain states and thus specific to resting-state fMRI, the network control framework is not specific to fMRI and could also be applied to other types of data. In this regard, the framework has already used to study brain states derived from electrocorticography (Stiso et al., 2019), and could also be imagined for electroencephalography data.

4.7.6 | Assessing structural connectivity through diffusion MRI

As the clinical dataset studied here was recorded as part of a large, longitudinal study for which the first scans were recorded more than 10 years ago, the diffusion MRI sequence constitutes a limiting factor. While motion may have had an influence on our result (Baum et al., 2018), only one b0 image was recorded in our diffusion MRI sequence, which made it impossible to estimate motion over the scanning duration. Therefore, motion may represent a confounding factor in our analysis that could not be quantified. Of note, another study investigating control energy who did control for motion also found decreasing control energy from childhood to adulthood (Cui et al., 2020), which suggests that in-scanner head motion was likely

not a major confound in our study. To overcome limitations regarding streamline reconstruction to assess structural connectivity, we used tractography based on fiber orientation distribution and CSD (Tournier et al., 2007, 2012, 2013), in combination with SIFT to increase biological accuracy (Smith et al., 2013). Therefore, we think that our streamline measure is a useful approach to estimate structural connectivity from the diffusion-weighted images in this dataset. Of note, we also replicated our results using streamline counts controlled for relative region size (see Figure S6). However, there remain the general limitations related to diffusion imaging for structural connectivity reconstruction, and our results should be replicated in future studies using more advanced diffusion image acquisition protocols that allow for a better consideration of confounding factors.

4.7.7 | Non-neural confounds in fMRI measurements

It is well-established that non-neural sources like heartbeat, respiration and motion can influence results of fMRI measurements. As motion is correlated with symptoms severity, it remains a possible confound in our study. We accounted for motion through common cleaning procedures such as regression of CSF and WM signals, followed by motion censoring. Of note, the regularized deconvolution from the hemodynamic response function in the iCAPs framework additionally minimizes effects caused by non-neural sources, as it filters out signals that do not follow the hemodynamic response function (Karahanoglu et al., 2013). In our previous study conducted in a largely overlapping sample, we have investigated the effect of motion in HCs and did not find any effect of motion on the iCAPs activation duration (Zöller et al., 2019), which suggests that it was not a large confound in the present study neither. However, as motion in patients is correlated to symptoms severity, it is not possible to perfectly untie the two effects, which remains a limitation of our study.

5 | CONCLUSION

In this study, we investigated the control energy of functional brain states in patients with 22q11DS. This is the first study investigating the impact of aberrant structural connectivity on brain function using control energy in 22q11DS. We found that altered connectivity in patients with 22q11DS leads to reduced energy impact for engaging frontal brain states, whereas more occipital and parietal brain states were energetically more demanding for patients with 22q11DS than HCs. Further, in a comparison of structural persistence control energy with resting-state fMRI activation, we found that the brain reduces energy by engaging less in energetically demanding brain states. In patients with 22q11DS the anticorrelation between activation and control energy is weaker than in controls, suggesting an ineffectiveness in reducing energy through cost-effective brain state activation in these patients. In summary, we contribute one of the first studies investigating a direct link between control energy and functional activation during rest and provide promising insights for a better understanding of brain alterations in 22q11DS.

5.1 | DIVERSITY STATEMENT

Recent work in several fields of science has identified a bias in citation practices such that papers from women and other minorities are under-cited relative to the number of such articles in the field (Caplar, Tacchella, & Birrer, 2017; Dion, Sumner, & Mitchell, 2018; Dworkin et al., 2020; Maliniak, Powers, & Walter, 2013; Mitchell, Lange, & Brus, 2013). Here, we sought to proactively consider choosing references that reflect the diversity of the field in thought, form of contribution, gender, and other factors. We obtained predicted gender of the first and last author of each reference by using databases that store the probability of a name being carried by a woman (Dworkin et al., 2020; Zhou et al., 2020). By this measure (and excluding self-citations to the first and last authors of our current article), our references contain 18.29% woman(first)/woman(last), 19.05% man/-woman, 17.12% woman/man, and 45.54% man/man. Second, we obtained predicted racial/ethnic category of the first and last author of each reference by databases that store the probability of a first and last name being carried by an author of color (Ambekar, Ward, Mohammed, Male, & Skiena, 2009; Sood & Laohaprapanon, 2018). By this measure (and excluding self-citations), our references contain 12.05% author of color (first)/author of color(last), 17.35% white author/author of color, 21.26% author of color/white author, and 49.35% white author/white author. This method is limited in that (a) names and Florida Voter Data to make the predictions may not be indicative of racial/ethnic identity and (b) it cannot account for Indigenous and mixed-race authors, or those who may face differential biases due to the ambiguous racialization or ethnicization of their names. We look forward to future work that could help us to better understand how to support equitable practices in science.

ACKNOWLEDGMENTS

The authors thank Jason Z. Kim for his advice and help with implementing the persistence control energy calculation. Further, we are grateful to the subjects who participated in our study and thank Sarah Menghetti, Léa Chambaz, Virginie Pouillard, and Dr. Maude Schneider for their involvement with the participants. The authors would also like to acknowledge Prof. François Lazeyras and the CIBM group for their support during data collection. This work was supported by the Swiss National Science Foundation (SNSF) under Grants 32473B_121966, 234730_144260, and 145250 to Stephan Eliez, and Grant 163859 to Marie Schaer, and by the National Center of Competence in Research (NCCR) "SYNAPSY—The Synaptic Bases of Mental Diseases," SNSF, under Grants 51AU40_125759, 51NF40_158776, and 51NF40-185897. DSB acknowledges support from the John D. and Catherine T. MacArthur Foundation, the Alfred P. Sloan Foundation, the ISI Foundation, the Paul Allen Foundation, the Army Research Laboratory (W911NF-10-2-0022), the Army Research Office (Bassett-W911NF-14-1-0679, DCIST- W911NF-

17-2-0181, W911NF-16-1-0474), the National Institute of Mental Health (2-R01-DC-009209-11, R01-MH112847, R01-MH107235, R21-M MH-106799), the National Institute of Child Health and Human Development (1R01HD086888-01), the National Institute of Neurological Disorders and Stroke (R01 NS099348), and the National Science Foundation (BCS-1441502, BCS-1430087, NSF PHY-1554488, and BCS-1631550). The content is solely the responsibility of the authors and does not necessarily represent the official views of any of the funding agencies.

CONFLICT OF INTEREST

The authors have no conflict of interest to declare.

DATA AVAILABILITY STATEMENT

The data that support the findings of this study are available on request from the corresponding author. The data are not publicly available due to privacy or ethical restrictions.

ORCID

Daniela Zöller https://orcid.org/0000-0002-7049-0696
Danielle S. Bassett https://orcid.org/0000-0002-6183-4493

REFERENCES

Aleman-Gomez, Y., Melie-García, L., & Valdés-Hernandez, P. (2006). *IBASPM: Toolbox for Automatic Parcellation of Brain Structures*. 12th Annual Meeting of the Organization for Human Brain Mapping.

Ambekar, A., Ward, C., Mohammed, J., Male, S., & Skiena, S. (2009). *Name-ethnicity Classification from Open Sources*. Proceedings of the ACM SIGKDD International Conference on Knowledge Discovery and Data Mining, pp. 49–57. doi: https://doi.org/10.1145/1557019.1557032.

Antsaklis, P. J., & Michel, A. N. (2005). *Linear systems*. Boston: Birkhäuser.

Ashburner, J. (2007). A fast diffeomorphic image registration algorithm. *NeuroImage*, *38*(1), 95–113. https://doi.org/10.1016/j.neuroimage.2007.07.007

Ashburner, J., & Friston, K. J. (2005). Unified segmentation. *NeuroImage*, *26*(3), 839–851. https://doi.org/10.1016/j.neuroimage.2005.02.018

Bassett, A. S., & Chow, E. W. C. (1999). 22q11 deletion syndrome: A genetic subtype of schizophrenia. *Biological Psychiatry*, *46*(7), 882–891. https://doi.org/10.1016/S0006-3223(99)00114-6

Bassett, D. S., & Sporns, O. (2017). Network neuroscience. *Nature Neuroscience*, *20*(3), 353–364. https://doi.org/10.1038/nn.4502

Bassett, D. S., Zurn, P., & Gold, J. I. (2018). On the nature and use of models in network neuroscience. *Nature Reviews Neuroscience*, *19*(9), 566–578. https://doi.org/10.1038/s41583-018-0038-8

Baum, G. L., Roalf, D. R., Cook, P. A., Ciric, R., Rosen, A. F., Xia, C., … Satterthwaite, T. D. (2018). The impact of in-scanner head motion on structural connectivity derived from diffusion MRI. *NeuroImage*, *173* (November 2017), 275–286. https://doi.org/10.1016/j.neuroimage.2018.02.041

Becker, C. O., Pequito, S., Pappas, G. J., Miller, M. B., Grafton, S. T., Bassett, D. S., & Preciado, V. M. (2018). Spectral mapping of brain functional connectivity from diffusion imaging. *Scientific Reports*, *8*(1), 1–15. https://doi.org/10.1038/s41598-017-18769-x

Bernhardt, B. C., Fadaie, F., Liu, M., Caldairou, B., Gu, S., Jefferies, E., … Bernasconi, N. (2019). Temporal lobe epilepsy: Hippocampal pathology modulates connectome topology and controllability. *Neurology*, *92* (19), E2209–E2220.

Betzel, R. F., Gu, S., Medaglia, J. D., Pasqualetti, F., & Bassett, D. S. (2016). Optimally controlling the human connectome: The role of network topology. *Scientific Reports*, *6*, 1–14. https://doi.org/10.1038/srep30770

Braun, U., Harneit, A., Pergola, G., Merana, T., Schaefer, A., Betzel, R., …, Tost, H. (2019). Brain state stability during working memory is explained by network control theory, modulated by dopamine D1/D2 receptor function, and diminished in schizophrenia. *bioRxiv preprint*, 679670. doi: https://doi.org/10.1101/679670.

Braun, U., Schaefer, A., Betzel, R. F., Tost, H., Meyer-Lindenberg, A., & Bassett, D. S. (2018). From maps to multi-dimensional network mechanisms of mental disorders. *Neuron*, *97*(1), 14–31. https://doi.org/10.1016/j.neuron.2017.11.007

Braun, U., Schäfer, A., Bassett, D. S., Rausch, F., Schweiger, J. I., Bilek, E., … Tost, H. (2016). Dynamic brain network reconfiguration as a potential schizophrenia genetic risk mechanism modulated by NMDA receptor function. *Proceedings of the National Academy of Sciences*, *113*(44), 12568–12573. https://doi.org/10.1073/pnas.1608819113

Caplar, N., Tacchella, S., & Birrer, S. (2017). Quantitative evaluation of gender bias in astronomical publications from citation counts. *Nature Astronomy*, *1*(6), 141.

Christoff, K., Irving, Z. C., Fox, K. C. R., Spreng, R. N., & Andrews-Hanna, J. R. (2016). Mind-wandering as spontaneous thought: A dynamic framework. *Nature Reviews Neuroscience*, *17*(11), 718–731. https://doi.org/10.1038/nrn.2016.113

Cole, M. W., Ito, T., Bassett, D. S., & Schultz, D. H. (2016). Activity flow over resting-state networks shapes cognitive task activations. *Nature Neuroscience*, *19*(12), 1718–1726. https://doi.org/10.1038/nn.4406

Cornblath, E. J., Ashourvan, A., Kim, J. Z., Betzel, R. F., Ciric, R., Adebimpe, A., … Bassett, D. S. (2020). Temporal sequences of brain activity at rest are constrained by white matter structure and modulated by cognitive demands. *Communications Biology*, *3*(261), 261. https://doi.org/10.1038/s42003-020-0961-x

Cornblath, E. J., Tang, E., Baum, G. L., Moore, T. M., Adebimpe, A., Roalf, D. R., … Bassett, D. S. (2018). Sex differences in network controllability as a predictor of executive function in youth. *NeuroImage*, *188*, 122–134. https://doi.org/10.1016/j.neuroimage.2018.11.048

Cui, Z., Stiso, J., Baum, G. L., Kim, J. Z., Roalf, D. R., Betzel, R. F., … Satterthwaite, T. D. (2020). Optimization of energy state transition trajectory supports the development of executive function during youth. *eLife*, *9*, 1–60. https://doi.org/10.7554/eLife.53060

Deco, G., Cruzat, J., Cabral, J., Knudsen, G. M., Carhart-Harris, R. L., Whybrow, P. C., … Kringelbach, M. L. (2018). Whole-brain multimodal neuroimaging model using serotonin receptor maps explains non-linear functional effects of LSD. *Current Biology*, *28*(19), 3065–3074. https://doi.org/10.1016/j.cub.2018.07.083

Dion, M. L., Sumner, J. L., & Mitchell, S. M. (2018). Gendered citation patterns across political science and social science methodology fields. *Political Analysis*, *26*(3), 312–327.

Du, Y., Pearlson, G. D., Yu, Q., He, H., Lin, D., Sui, J., … Calhoun, V. D. (2016). Interaction among subsystems within default mode network diminished in schizophrenia patients: A dynamic connectivity approach. *Schizophrenia Research*, *170*(1), 55–65. https://doi.org/10.1016/j.schres.2015.11.021

Dworkin, J. D., Linn, K. A., Teich, E. G., Zurn, P., Shinohara, R. T., & Bassett, D. S. (2020). The extent and drivers of gender imbalance in neuroscience reference lists. *Nature Neuroscience*, *23*, 918–926. https://doi.org/10.1101/2020.01.03.894378

Etkin, A., & Wager, T. (2007). Reviews and overviews functional neuroimaging of anxiety: A meta-analysis of emotional processing in PTSD, social anxiety disorder, and specific phobia. *The American Journal of Psychiatry*, *164*(October), 1476–1488. https://doi.org/10.1078/1439-1791-00175

Farouj, Y., Karahanoglu, F. I., & Van De Ville, D. (2017). *Regularized Spatio-temporal Deconvolution of fMRI Data Using Gray-Matter Constrained Total Variation*. Proceedings of the 14th IEEE International Symposium on Biomedical Imaging: From Nano to Macro (ISBI'17), pp. 472–475.

Fornito, A., Zalesky, A., Pantelis, C., & Bullmore, E. T. (2012). Schizophrenia, neuroimaging and connectomics. *NeuroImage*, *62*(4), 2296–2314. https://doi.org/10.1016/j.neuroimage.2011.12.090

Friston, K., Brown, H. R., Siemerkus, J., & Stephan, K. E. (2016). The dysconnection hypothesis (2016). *Schizophrenia Research*, *176*(2–3), 83–94. https://doi.org/10.1016/j.schres.2016.07.014

Fusar-Poli, P., Borgwardt, S., Bechdolf, A., Addington, J., Riecher-Rössler, A., Schultze-Lutter, F., … Yung, A. (2013). The psychosis high-risk state. *JAMA Psychiatry*, *70*(1), 107–120. https://doi.org/10.1001/jamapsychiatry.2013.269

Ghosh, A., Rho, Y., McIntosh, A. R., Kötter, R., & Jirsa, V. K. (2008). Noise during rest enables the exploration of the brain's dynamic repertoire. *PLoS Computational Biology*, *4*(10), e1000196. https://doi.org/10.1371/journal.pcbi.1000196

Gothelf, D., Hoeft, F., Ueno, T., Sugiura, L., Lee, A. D., Thompson, P., & Reiss, A. L. (2011). Developmental changes in multivariate neuroanatomical patterns that predict risk for psychosis in 22q11.2 deletion syndrome. *Journal of Psychiatric Research*, *45*(3), 322–331. https://doi.org/10.1016/j.jpsychires.2010.07.008

Gu, S., Betzel, R. F., Mattar, M. G., Cieslak, M., Delio, P. R., Grafton, S. T., … Bassett, D. S. (2017). Optimal trajectories of brain state transitions. *NeuroImage*, *148*(January), 305–317. https://doi.org/10.1016/j.neuroimage.2017.01.003

Gu, S., Pasqualetti, F., Cieslak, M., Telesford, Q. K., Yu, A. B., Kahn, A. E., … Bassett, D. S. (2015). Controllability of structural brain networks. *Nature Communications*, *6*, 8414. https://doi.org/10.1038/ncomms9414

Hasenkamp, W., James, G. A., Boshoven, W., & Duncan, E. (2011). Altered engagement of attention and default networks during target detection in schizophrenia. *Schizophrenia Research*, *125*(2–3), 169–173. https://doi.org/10.1016/j.schres.2010.08.041

Honey, C. J., Sporns, O., Cammoun, L., Gigandet, X., Thiran, J.-P., Meuli, R., & Hagmann, P. (2009). Predicting human resting-state functional connectivity from structural connectivity. *Proceedings of the National Academy of Sciences of the United States of America*, *106*(6), 2035–2040. https://doi.org/10.1073/pnas.0811168106

Insel, T. R. (2010). Rethinking schizophrenia. *Nature*, *468*(7321), 187–193. https://doi.org/10.1038/nature09552

Jeganathan, J., Perry, A., Bassett, D. S., Roberts, G., Mitchell, P. B., & Breakspear, M. (2018). Fronto-limbic dysconnectivity leads to impaired brain network controllability in young people with bipolar disorder and those at high genetic risk. *NeuroImage: Clinical*, *19*(March), 71–81. https://doi.org/10.1016/j.nicl.2018.03.032

Jenkinson, M., Bannister, P., Brady, M., & Smith, S. (2002). Improved optimization for the robust and accurate linear registration and motion correction of brain images. *NeuroImage*, *17*(2), 825–841. https://doi.org/10.1006/nimg.2002.1132

Jenkinson, M., Beckmann, C. F., Behrens, T. E., Woolrich, M. W., & Smith, S. M. (2012). FSL. *NeuroImage*, *62*(2), 782–790. https://doi.org/10.1016/j.neuroimage.2011.09.015

Karahanoglu, F. I., Bayram, I., & Van De Ville, D. (2011). A signal processing approach to generalized 1-D total variation. *IEEE Transactions on Signal Processing*, *59*(11), 5265–5274.

Karahanoglu, F. I., Caballero-Gaudes, C., Lazeyras, F., & Van De Ville, D. (2013). Total activation: FMRI deconvolution through spatio-temporal regularization. *NeuroImage*, *73*, 121–134. https://doi.org/10.1016/j.neuroimage.2013.01.067

Karahanoglu, F. I., & Van De Ville, D. (2015). Transient brain activity disentangles fMRI resting-state dynamics in terms of spatially and temporally overlapping networks. *Nature Communications*, *6*, 7751. https://doi.org/10.1038/ncomms8751

Karahanoğlu, F. I., & Van De Ville, D. (2017). Dynamics of large-scale fMRI networks: Deconstruct brain activity to build better models of brain function. *Current Opinion in Biomedical Engineering*, *3*, 28–36. https://doi.org/10.1016/j.cobme.2017.09.008

Karrer, T. M., Kim, J. Z., Stiso, J., Kahn, A. E., Pasqualetti, F., Habel, U., & Bassett, D. S. (2020). A practical guide to methodological considerations in the controllability of structural brain networks. *Journal of Neural Engineering*, *17*(2), 026031. https://doi.org/10.1088/1741-2552/ab6e8b

Khambhati, A. N., Kahn, A. E., Costantini, J., Ezzyat, Y., Solomon, E. A., Gross, R. E., … Bassett, D. S. (2019). Functional control of electrophysiological network architecture using direct neurostimulation in humans. *Network Neuroscience*, *3*(3), 848–877. https://doi.org/10.1162/netn_a_00089

Kikinis, Z., Cho, K. I. K., Coman, I. L., Radoeva, P. D., Bouix, S., Tang, Y., … Kates, W. R. (2016). Abnormalities in brain white matter in adolescents with 22q11.2 deletion syndrome and psychotic symptoms. *Brain Imaging and Behavior*, *11*(5), 1353–1364. https://doi.org/10.1007/s11682-016-9602-x

Kikinis, Z., Makris, N., Finn, C. T., Bouix, S., Lucia, D., Coleman, M. J., … Kubicki, M. (2013). Genetic contributions to changes of fiber tracts of ventral visual stream in 22q11.2 deletion syndrome. *Brain Imaging and Behavior*, *7*(3), 316–325. https://doi.org/10.1007/s11682-013-9232-5

Kim, J. Z. & Bassett, D. S. (2019). Linear dynamics & control of brain networks. *arXiv preprint*, 1902.03309:1–30.

Kim, J. Z., Soffer, J. M., Kahn, A. E., Vettel, J. M., Pasqualetti, F., & Bassett, D. S. (2018). Role of graph architecture in controlling dynamical networks with applications to neural systems. *Nature Physics*, *14*(1), 91–98. https://doi.org/10.1038/nphys4268

Klein, A., Andersson, J., Ardekani, B. A., Ashburner, J., Avants, B., Chiang, M. C., … Parsey, R. V. (2009). Evaluation of 14 nonlinear deformation algorithms applied to human brain MRI registration. *NeuroImage*, *46*(3), 786–802. https://doi.org/10.1016/j.neuroimage.2008.12.037

Kringelbach, M. L., Cruzat, J., Cabral, J., Knudsen, G. M., Carhart-Harris, R., Whybrow, P. C., … Deco, G. (2020). Dynamic coupling of whole-brain neuronal and neurotransmitter systems. *Proceedings of the National Academy of Sciences of the United States of America*, *117*(17), 9566–9576. https://doi.org/10.1073/pnas.1921475117

Krishnan, A., Williams, L. J., McIntosh, A. R., & Abdi, H. (2011). Partial least squares (PLS) methods for neuroimaging: A tutorial and review. *NeuroImage*, *56*(2), 455–475. https://doi.org/10.1016/j.neuroimage.2010.07.034

Lee, W. H., Rodrigue, A., Glahn, D. C., Bassett, D. S., & Frangou, S. (2020). Heritability and cognitive relevance of structural brain controllability. *Cerebral Cortex*, *30*(5), 3044–3054. https://doi.org/10.1093/cercor/bhz293

Lynn, C. W., & Bassett, D. S. (2019). The physics of brain network structure, function and control. *Nature Reviews Physics*, *1*(5), 318–332. https://doi.org/10.1038/s42254-019-0040-8

Maeder, J., Schneider, M., Bostelmann, M., Debbané, M., Glaser, B., Menghetti, S., … Eliez, S. (2016). Developmental trajectories of executive functions in 22q11.2 deletion syndrome. *Journal of Neurodevelopmental Disorders*, *8*(1), 10. https://doi.org/10.1186/s11689-016-9141-1

Maliniak, D., Powers, R., & Walter, B. F. (2013). The gender citation gap in international relations. *International Organization*, *67*(4), 889–922.

Mancini, V., Sandini, C., Padula, M. C., Zöller, D., Schneider, M., Schaer, M., & Eliez, S. (2019). Positive psychotic symptoms are associated with divergent developmental trajectories of hippocampal volume during late adolescence in patients with 22q11DS. *Molecular Psychiatry*, *25*, 2844–2859. https://doi.org/10.1038/s41380-019-0443-z

McDonald-McGinn, D. M., Sullivan, K. E., Marino, B., Philip, N., Swillen, A., Vorstman, J. A. S., … Bassett, A. S. (2015). 22q11.2 deletion syndrome. *Nature Reviews Disease Primers*, *1*, 15071.

Menon, V. (2011). Large-scale brain networks and psychopathology: A unifying triple network model. *Trends in Cognitive Sciences*, *15*(10), 483–506. https://doi.org/10.1016/j.tics.2011.08.003

Miller, T. J., Mcqlashan, T. H., Rosen, J. L., Cadenhead, K., Ventura, J., Mcfarlane, W., … Woods, S. W. (2003). Prodromal assessment with the structured interview for prodromal syndromes and the scale of prodromal symptoms: Predictive validity, Interrater reliability, and training to reliability. *Schizophrenia Bulletin*, *29*(4), 703–715. https://doi.org/10.1093/oxfordjournals.schbul.a007040

Mitchell, S. M., Lange, S., & Brus, H. (2013). Gendered citation patterns in international relations journals. *International Studies Perspectives*, *14*(4), 485–492.

Monti, S., Tamayo, P., Mesirov, J., & Golub, T. (2003). Consensus clustering: A resampling-based method for class discovery and visualization of gene expression microarray data. *Machine Learning*, *52*(1), 91–118. https://doi.org/10.1023/A:1023949509487

Muldoon, S. F., Pasqualetti, F., Gu, S., Cieslak, M., Grafton, S. T., Vettel, J. M., and Bassett, D. S. (2016). Stimulation-based control of dynamic brain networks. *PLoS Computational Biology*, *12*(9):e1005076. doi: https://doi.org/10.1109/TAC.2015.2496191, 2591, 2596

Olszewski, A. K., Kikinis, Z., Gonzalez, C. S., Coman, I. L., Makris, N., Gong, X., … Kates, W. R. (2017). The social brain network in 22q11.2 deletion syndrome: A diffusion tensor imaging study. *Behavioral and Brain Functions*, *13*(1), 1–17. https://doi.org/10.1186/s12993-017-0122-7

Ottet, M.-C., Schaer, M., Cammoun, L., Schneider, M., Debbané, M., Thiran, J.-P., & Eliez, S. (2013). Reduced fronto-temporal and limbic connectivity in the 22q11.2 deletion syndrome: Vulnerability markers for developing schizophrenia? *PLoS One*, *8*(3), e58429. https://doi.org/10.1371/journal.pone.0058429

Ottet, M.-C., Schaer, M., Debbané, M., Cammoun, L., Thiran, J.-P., & Eliez, S. (2013). Graph theory reveals dysconnected hubs in 22q11DS and altered nodal efficiency in patients with hallucinations. *Frontiers in Human Neuroscience*, *7*(September), 402. https://doi.org/10.3389/fnhum.2013.00402

Padula, M. C., Scariati, E., Schaer, M., & Eliez, S. (2018). A mini review on the contribution of the anterior cingulate cortex in the risk of psychosis in 22q11.2 deletion syndrome. *Frontiers in Psychiatry*, *9*(August), 9–14. https://doi.org/10.3389/fpsyt.2018.00372

Padula, M. C., Scariati, E., Schaer, M., Sandini, C., Ottet, M. C., Schneider, M., … Eliez, S. (2017). Altered structural network architecture is predictive of the presence of psychotic symptoms in patients with 22q11.2 deletion syndrome. *NeuroImage: Clinical*, *16*(July), 142–150. https://doi.org/10.1016/j.nicl.2017.07.023

Padula, M. C., Schaer, M., Scariati, E., Maeder, J., Schneider, M., & Eliez, S. (2017). Multimodal investigation of triple network connectivity in patients with 22q11DS and association with executive functions. *Human Brain Mapping*, *2189*(January), 2177–2189. https://doi.org/10.1002/hbm.23512

Padula, M. C., Schaer, M., Scariati, E., Schneider, M., Van De Ville, D., Debbané, M., & Eliez, S. (2015). Structural and functional connectivity in the default mode network in 22q11.2 deletion syndrome. *Journal of Neurodevelopmental Disorders*, *7*(1), 23. https://doi.org/10.1186/s11689-015-9120-y

Preti, M. G., Bolton, T. A. W., & Van De Ville, D. (2017). The dynamic functional connectome: State-of-the-art and perspectives. *NeuroImage*, *160*(December), 41–54. https://doi.org/10.1016/j.neuroimage.2016.12.061

Roalf, D. R., Eric Schmitt, J., Vandekar, S. N., Satterthwaite, T. D., Shinohara, R. T., Ruparel, K., … Gur, R. E. (2017). White matter microstructural deficits in 22q11.2 deletion syndrome. *Psychiatry Research: Neuroimaging*, *268*(March), 35–44. https://doi.org/10.1016/j.pscychresns.2017.08.001

Rubinov, M., & Sporns, O. (2010). Complex network measures of brain connectivity: Uses and interpretations. *NeuroImage*, *52*(3), 1059–1069. https://doi.org/10.1016/j.neuroimage.2009.10.003

Scariati, E., Padula, M. C., Schaer, M., & Eliez, S. (2016). Long-range dysconnectivity in frontal and midline structures is associated to psychosis in 22q11.2 deletion syndrome. *Journal of Neural Transmission*, *123*, 823–839. https://doi.org/10.1007/s00702-016-1548-z

Schneider, M., Debbané, M., Bassett, A. S., Chow, E. W. C., Fung, W. L. A., van den Bree, M. B. M., … Eliez, S. (2014). Psychiatric disorders from childhood to adulthood in 22q11.2 deletion syndrome: Results from the international consortium on brain and behavior in 22q11.2 deletion syndrome. *The American Journal of Psychiatry*, *171*(6), 627–639. https://doi.org/10.1176/appi.ajp.2013.13070864

Schreiner, M. J., Karlsgodt, K. H., Uddin, L. Q., Chow, C., Congdon, E., Jalbrzikowski, M., & Bearden, C. E. (2014). Default mode network connectivity and reciprocal social behavior in 22q11.2 deletion syndrome. *Social Cognitive and Affective Neuroscience*, *9*(9), 1261–1267. https://doi.org/10.1093/scan/nst114

Shine, J. M., Breakspear, M., Bell, P. T., Ehgoetz Martens, K., Shine, R., Koyejo, O., … Poldrack, R. A. (2019). Human cognition involves the dynamic integration of neural activity and neuromodulatory systems. *Nature Neuroscience*, *22*(2), 289–296. https://doi.org/10.1038/s41593-018-0312-0

Smith, R. E., Tournier, J. D., Calamante, F., & Connelly, A. (2013). SIFT: Spherical-deconvolution informed filtering of tractograms. *NeuroImage*, *67*, 298–312. https://doi.org/10.1016/j.neuroimage.2012.11.049

Sood, G. & Laohaprapanon, S. (2018). Predicting race and ethnicity from the sequence of characters in a name. *arXiv preprint*, page 1805.02109.

Srivastava, P., Nozari, E., Kim, J. Z., Ju, H., Zhou, D., Becker, C., … Bassett, D. S. (2020). Models of communication and control for brain networks: Distinctions, convergence, and future outlook. *Network Neuroscience*, *4*(4), 1122–1159. https://doi.org/10.1162/netn_a_00158.

Stiso, J., Khambhati, A. N., Menara, T., Kahn, A. E., Stein, J. M., Das, S. R., … Bassett, D. S. (2019). White matter network architecture guides direct electrical stimulation through optimal state transitions. *Cell Reports*, *28*(10), 2554–2566.e7. https://doi.org/10.1016/j.celrep.2019.08.008

Tang, E., & Bassett, D. S. (2018). Colloquium: Control of dynamics in brain networks. *Reviews of Modern Physics*, *90*(3), 1–20. https://doi.org/10.1103/RevModPhys.90.031003

Tang, E., Giusti, C., Baum, G. L., Gu, S., Pollock, E., Kahn, A. E., … Bassett, D. S. (2017). Developmental increases in white matter network controllability support a growing diversity of brain dynamics. *Nature Communications*, *8*(1), 1252. https://doi.org/10.1038/s41467-017-01254-4

Tournier, J. D., Calamante, F., & Connelly, A. (2007). Robust determination of the fibre orientation distribution in diffusion MRI: Non-negativity constrained super-resolved spherical deconvolution. *NeuroImage*, *35*(4), 1459–1472. https://doi.org/10.1016/j.neuroimage.2007.02.016

Tournier, J. D., Calamante, F., & Connelly, A. (2012). MRtrix: Diffusion tractography in crossing fiber regions. *International Journal of Imaging Systems and Technology*, *22*(1), 53–66. https://doi.org/10.1002/ima.22005

Tournier, J. D., Calamante, F., & Connelly, A. (2013). Determination of the appropriate b value and number of gradient directions for high-angular-resolution diffusion-weighted imaging. *NMR in Biomedicine*, *26*(12), 1775–1786. https://doi.org/10.1002/nbm.3017

Tournier, J. D., Smith, R. E., Raffelt, D. A., Tabbara, R., Dhollander, T., Pietsch, M., …, Connelly, A. (2019). MRtrix3: A fast, flexible and open software framework for medical image processing and visualisation. *bioRxiv preprint*, 551739. doi: https://doi.org/10.1101/551739.

Tylee, D. S., Kikinis, Z., Quinn, T. P., Antshel, K. M., Fremont, W., Tahir, M. A., … Makris, N. (2017). Machine-learning classification of 22q11.2 deletion syndrome: A diffusion tensor imaging study. *NeuroImage: Clinical*, *15*(March), 832–842. https://doi.org/10.1016/j.nicl.2017.04.029

Van Den Heuvel, M. P., & Fornito, A. (2014). Brain networks in schizophrenia. *Neuropsychology Review*, *24*(1), 32–48. https://doi.org/10.1007/s11065-014-9248-7

Váša, F., Griffa, A., Scariati, E., Schaer, M., Urben, S., Eliez, S., & Hagmann, P. (2016). An affected core drives network integration deficits of the structural connectome in 22q11.2 deletion syndrome. *NeuroImage: Clinical*, *10*, 239–249. https://doi.org/10.1016/j.nicl.2015.11.017

Wechsler, D. (1991). *Weschler intelligence scale for children*. San Antonio, TX: Psychological Corporation.

Wechsler, D. (1997). *Wechsler intelligence scale for adults*. London: The Psychological Corporation.

Westfall, P. H., & Young, S. S. (1993). *Resampling-based multiple testing: Examples and methods for p-value adjustment* (Vol. 279). Hoboken, NJ: John Wiley & Sons.

Wu-Yan, E., Betzel, R. F., Tang, E., Gu, S., Pasqualetti, F., & Bassett, D. S. (2018). Benchmarking measures of network controllability on canonical graph models. *Journal of Nonlinear Science*, *30*, 1–39. https://doi.org/10.1007/s00332-018-9448-z

Yan, C., & Yufeng, Z. (2010). DPARSF: A MATLAB toolbox for "pipeline" data analysis of resting-state fMRI. *Frontiers in System Neuroscience*, *4*, 13. https://doi.org/10.3389/fnsys.2010.00013

Zhan, L., Jenkins, L. M., Zhang, A., Conte, G., Forbes, A., Harvey, D., … Simon, T. J. (2018). Baseline connectome modular abnormalities in the childhood phase of a longitudinal study on individuals with chromosome 22q11.2 deletion syndrome. *Human Brain Mapping*, *39*(1), 232–248. https://doi.org/10.1002/hbm.23838

Zhou, D., Cornblath, E. J., Stiso, J., Teich, E. G., Dworkin, J. D., Blevins, A. S., & Bassett, D. S. (2020). Gender Diversity Statement and Code Notebook v1.0.

Zöller, D., Bolton, T. A., Karahanoglu, F. I., Eliez, S., Schaer, M., & Van De Ville, D. (2018). Robust recovery of temporal overlap between network activity using transient-informed spatio-temporal regression. *IEEE Transactions on Medical Imaging*, *38*(1), 291–302. https://doi.org/10.1109/TMI.2018.2863944

Zöller, D., Padula, M. C., Sandini, C., Schneider, M., Scariati, E., Van De Ville, D., … Eliez, S. (2017). Psychotic symptoms influence the development of anterior cingulate BOLD variability in 22q11.2 deletion syndrome. *Schizophrenia Research*, *193*, 319–328. https://doi.org/10.1016/j.schres.2017.08.003

Zöller, D., Sandini, C., Karahanoğlu, F. I., Padula, M. C., Schaer, M., Eliez, S., & Van De Ville, D. (2019). Large-scale brain network dynamics provide a measure of psychosis and anxiety in 22q11.2 deletion syndrome. *Biological Psychiatry: Cognitive Neuroscience and Neuroimaging*, *4*(10), 881–892. https://doi.org/10.1016/j.bpsc.2019.04.004

Zöller, D., Schaer, M., Scariati, E., Padula, M. C., Eliez, S., & Van De Ville, D. (2017). Disentangling resting-state BOLD variability and PCC functional connectivity in 22q11.2 deletion syndrome. *NeuroImage*, *149* (January), 85–97. https://doi.org/10.1016/j.neuroimage.2017.01.064

SUPPORTING INFORMATION

Additional supporting information may be found online in the Supporting Information section at the end of this article.

How to cite this article: Zöller D, Sandini C, Schaer M, Eliez S, Bassett DS, Van De Ville D. Structural control energy of resting-state functional brain states reveals less cost-effective brain dynamics in psychosis vulnerability. *Hum Brain Mapp*. 2021;42:2181–2200. https://doi.org/10.1002/hbm.25358